CHAPTER 1

Introduction

Diamond together with a few other materials can be used as a gem stone and as an industrial tool [1]. One of the most remarkable features of diamond is that it is pre-eminent in both of these fields, i.e. it is the most beautiful of all gem stones and the most powerful of all cutting materials. Natural diamond is predominantly used as gem stones, whilst synthetic diamond is used in industrial applications.

The two vital properties which make diamond so important as an industrial material are its combination of extreme hardness and high thermal conductivity [1]. Diamond possesses other technologically important properties such as high electrical resistance, chemical inertness, high electron and hole mobilities and optical transparency [2,3]. Diamond is chemically inert in a variety of environments including strong acids, bases, fluoride and chloride environments [4].

One of the techniques of manufacturing synthetic diamond is high pressure, high temperature synthesis, and the other is chemical vapour deposition (CVD) of diamond onto a substrate. The high pressure, high temperature route gives rise to single diamond crystals, whilst the CVD route produces diamond thin films. These films are deposited via two methods : hot filament chemical vapour deposition (HF-CVD) and microwave

assisted chemical vapour deposition (MA-CVD) (refer to Chapter 2). The as-grown diamond films are non-conductive, i.e. they are insulators. In order to enhance their conductivity, these synthetic diamond films are doped with boron.

There are many applications for boron-doped CVD diamond [5], such as :

- Electrosynthesis
- Corrosion protection
- Energy storage devices
- Electrochemical-based toxic waste remediation
- Detection of sodium azide in groundwater
- Anodic stripping voltammetry of heavy-metal ions in aqueous media

Another potential use for boron-doped CVD diamond is as a biosensor in biological systems. At present, there is a worldwide interest in the use of diamond thin films in electroanalysis [5-11]. Conducting diamond electrodes provide unique advantages for electrochemistry :

- Wide potential window of water stability
- Low background current density (low baseline current)
- Exceptional chemical and structural stability
- Resistance to fouling

The wide potential range of water stability at diamond electrodes permits reactants with large positive or negative standard potentials to be investigated on diamond without

interference from water electrolysis [12]. The low background current density also enables diamond to have a lower detection limit (higher signal/noise ratio) than most other materials.

In recent years, several groups have made progress understanding the factors that influence the electrochemical response of diamond thin film electrodes, including those of Fujishima and Yagi (Japan) [10], Pleskov (Russia) [13], Angus and Miller (USA) [11], Swain (USA) [8] and Compton (England) [14]. However, there can be significant variability in the response of the diamond electrodes, as reported in results from different laboratories. According to Swain et. al. [15], this variability can be ascribed to two sets of factors :

a) The solution condition, surface cleanliness, the redox analyte and the electrolyte composition
b) Diamond film quality issues

The factors that can influence the film quality are :

- Presence of non-diamond carbon
- The surface state of the diamond film, i.e. oxygen or hydrogen terminated surface
- Type of dopant, doping level and the distribution of the dopant in the diamond film
- Grain boundaries and other morphological defects
- The primary crystallographic orientation

1.1 Aim of investigation

The aim of this investigation was to study the electrochemical behaviour of boron-doped CVD diamond electrodes, in order to establish its potential use as a biosensor. Part of the study entailed a thorough literature survey on diamond electrodes, their properties and applications. Research work was carried out to characterise the diamond electrode in terms of its microstructure, quantity of non-diamond carbon present, boron concentration and surface chemistry. The techniques used were scanning electron microscopy (SEM), energy dispersive spectroscopy (EDS), Raman spectroscopy, laser ablation inductively coupled plasma mass spectroscopy (LA-ICP-MS) and X-ray photoelectron spectroscopy (XPS).

The surface of the electrode is deemed to be extremely important in determining the electrochemical behaviour of the diamond electrode in certain systems. The redox systems investigated were potassium iron (III) cyanide and cerium (III) sulphate, whilst the biological systems were dopamine and ascorbic acid. The electrode surface was therefore modified to become either oxygen terminated or hydrogen terminated, and the effect on the various systems was investigated.

Potassium iron (III) cyanide is a standard electrochemical system that is often used to determine the electrochemical behaviour of electrodes. The cerium redox couple is not very well resolved using a glassy carbon electrode. However, a fairly well resolved cerium redox couple is obtained using a boron-doped diamond electrode because of its

wide potential window. Dopamine is found in the brain fluid in conjunction with ascorbic acid (an interfering species). Literature reports that dopamine can be separated from ascorbic acid using an anodically pretreated boron-doped diamond electrode.

A voltammetric comparison of the diamond electrode with the glassy carbon electrode was also undertaken in these electrochemical systems, as the glassy carbon electrode is the most widely used commercial electrode with which diamond would have to compete. Lastly, the ability of the diamond electrode to detect the presence of thyroid hormones (L-T_3 and L-T_4) in synthetic samples was investigated in order to assess the feasibility of using diamond electrodes as immunosensors.

1.2 References

[1] R Berman, **Physical Properties of Diamond;** Clarendon Press, Oxford (1965).

[2] T D Moustakas, **In Synthetic Diamond : Emerging Science and Technology,** John Wiley and Sons, New York (1994) 145.

[3] C J Hartley and H L Shergold, **Chemistry and Industry**, (1980) 224.

[4] R Ramesham and M F Rose, **Journal of High Temperature and Materials Science, 38** (1997) 1.

[5] J Xu, M C Granger, Q Chen, J W Strojek, T E Lister and G M Swain, **Analytical Chemistry News & Features, 69** (1997) 591A.

[6] S Alehashem, F Chamber, J W Strojek, G M Swain and R Ramesham, **Anal. Chem., 67** (1995) 2812.

[7] S Jolley, M D Koppang, T Jackson and G M Swain, **Anal. Chem., 69** (1997) 4041.

[8] J Xu and G M Swain, **Anal. Chem., 70** (1998) 1502.

[9] M D Koppang, M Witek, J Blau and G M Swain, **Anal. Chem., 71** (1999) 1188.

[10] T N Rao, I Yagi, T Miwa, D A Tryk and A Fujishima, **Anal. Chem., 71** (1999) 2506.

[11] J C Angus, H B Martin, U Landau, Y E Evstefeeva, B Miller and N Vinokur, **New Diamond and Frontier Carbon Technology, 9** (1999) 175.

[12] A Argoitia, H B Martin, E J Rozak, U Landau and J L Angus, **Mater. Res. Soc. Proc., 416** (1996) 349.

[13] Y V Pleskov, **Russian Chemical Reviews, 68** (1999) 381.

[14] C H Goeting, F Marken, A Gutierrez-Sosa, R G Compton and J S Foord, **New Diamond and Frontier Carbon Technology, 9** (1999) 207.

[15] M C Granger, M Witek, J Xu, J Wang, M Hupert, A Hanks, M D Koppang, J E Butler, G Lucazeau, M Mermoux, J W Strojek and G M Swain, **Anal. Chem., 72** (2000) 3793.

CHAPTER 2

Manufacture of boron-doped CVD diamond

2.1 Introduction

The low pressure synthesis of diamond thin films by chemical vapour deposition (CVD) methods began about two decades ago. Chemical vapour deposition involves a gas-phase chemical reaction occurring above a solid surface, which causes deposition onto that surface [1]. The process gas usually used for the production of CVD diamond is a hydrocarbon gas, typically methane, in an excess of hydrogen.

In order to produce diamond films, the gas-phase carbon molecules need to be activated. This generally involves plasma (for example microwave) or thermal (for example hot filament) activation, or use of a combustion flame (oxyacetylene or plasma torches) [1]. The two most common low pressure CVD techniques are hot filament CVD and microwave plasma CVD. The grown CVD diamond can show mechanical and even electronic properties comparable to those of natural and high pressure, high temperature synthetic diamond.

2.2 Hot filament CVD and microwave plasma CVD techniques

One of the most commonly used substrates for the deposition of diamond film is the p-type (100) silicon wafer [2-5]. This substrate is usually scratched with diamond paste before deposition to increase the nucleation density of the diamond particles which make up the film. Typical growth conditions for the hot filament and microwave plasma CVD techniques are carbon/hydrogen volume ratios of 0.5 - 2%, pressures of 10 – 100 torr, substrate temperatures of 800 – 1000°C, and microwave powers of 1000 – 1300 W, or filament temperatures of approximately 2100°C, depending on the method used [6].

The most common method of incorporating boron into the diamond film is during the process of its growth. Since the boron atoms are almost the same magnitude as the carbon atoms, they are easily incorporated into the diamond lattice by substitution of a carbon atom. Boron doping of the diamond film can be accomplished by either supplementing the gas phase with a volatile boron compound, for example trimethyl borate, or by introducing the boron into the diamond film from the solid state by, for example, gasifying a piece of hexagonal – boron nitride (h-BN) or boron trioxide powder [7,8].

Figure 2.1 illustrates a schematic diagram of a hot filament CVD apparatus. A mixture of hydrogen and methane is introduced into the reaction chamber, while the rotary pump displaces the mixed gas in the chamber to balance the inside pressure. The bond of the gas molecules is broken by the thermal energy of a tungsten (W) filament and carbon atoms are deposited on the substrate located just below the filament. Boron trioxide

(B_2O_3) powder is placed in a quartz boat in the branch tube of the deposition chamber and heated electrically to the required temperature.

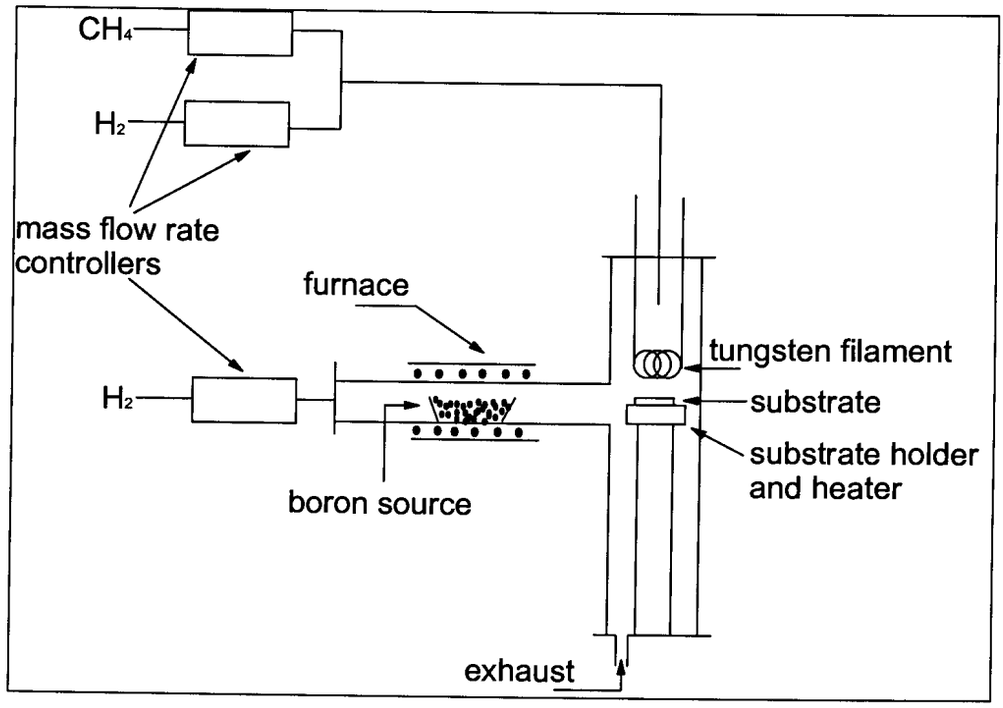

Figure 2.1 : Schematic diagram of a hot filament CVD apparatus [2]

Figure 2.2 represents a schematic diagram of a microwave plasma enhanced CVD reactor. The volatile boron compound is introduced with the reactant gas. This reactant gas is activated via microwaves that are generated by the microwave generator.

The morphology of the polycrystalline diamond films is sensitive to the precise growth conditions. Growth rates for the various deposition processes vary considerably, and it is usually found that the higher the growth rate of the film, the lower the quality [1]. The term "quality" refers to factors such as the ratio of sp^3 (diamond) to sp^2-bonded (graphite) carbon in the sample and the crystallinity of the film. The average growth rate of the hot

filament and plasma methods is 0.1 – 10 μm/h. One of the great challenges facing researchers in CVD diamond technology is to increase the growth rates to economically viable rates, that is hundreds of μm/h or even to mm/h, without compromising film quality.

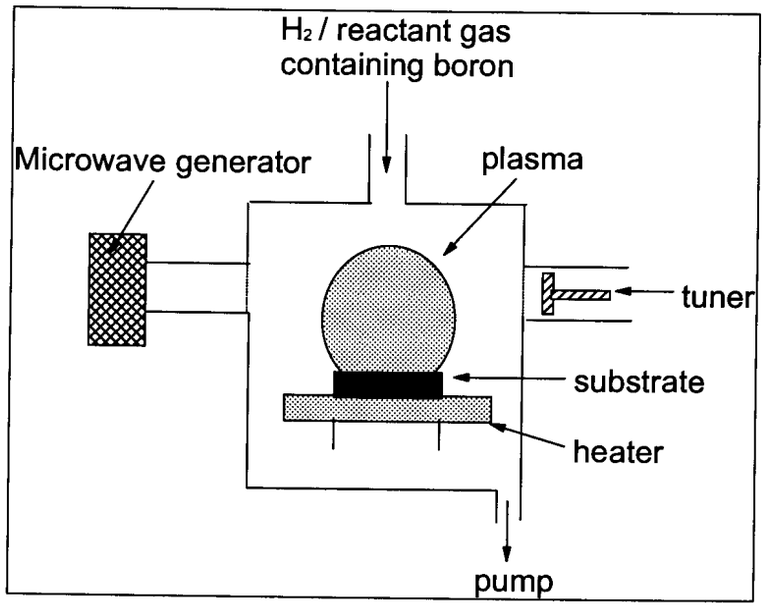

Figure 2.2 : Schematic diagram of a microwave plasma enhanced CVD reactor [1]

Graphite is the thermodynamically stable form of solid carbon at ambient pressures and temperatures. The fact that diamond films can be formed by CVD techniques is most probably linked to the presence of hydrogen atoms, which are generated by the activation of the gas molecules. These hydrogen atoms are believed to play a number of crucial roles in the CVD process [1] :

(a) They undergo hydrogen abstraction reactions with stable gas-phase hydrocarbon molecules, producing highly reactive carbon-containing radical species. This is

important, since stable hydrocarbon molecules do not react to cause diamond growth. The reactive radicals, for example methyl ($\cdot CH_3$), can thus diffuse to the substrate surface and react, forming the C-C bond necessary to propagate the diamond lattice.

(b) Hydrogen atoms prevent the reconstruction of the 'dangling' carbon bonds to a graphite-like surface by terminating these carbon bonds with hydrogen atoms on the growing diamond surface, thus hindering them from cross-linking.

(c) Atomic hydrogen is known to etch both diamond and graphite. Under typical CVD conditions, the rate of diamond growth exceeds its etch rate, whilst the converse is true for other forms of carbon, for example graphite. Thus, the atomic hydrogen, even though it is very short lived, is effective in etching out non-diamond particles. This is believed to be the basis for the preferential deposition of diamond rather than graphite.

2.3 Effect of varying deposition conditions on the morphology of CVD diamond

The surface morphology of CVD diamond was found to be dependent on the concentration of methane in the feed gas [9]. **Figure 2.3** shows typical examples of the morphology of as-grown surfaces as the concentration of methane in the feed gas is increased from 0.5% to 5.0%. Low methane concentrations, for example 0.5%, were found to yield (111) faces, whereas methane concentrations greater than 1.5% yielded (100) faces. The (100) faces occurred as square or rectangular forms. For the films grown at a 5% methane concentration, the crystalline morphology was entirely lost.

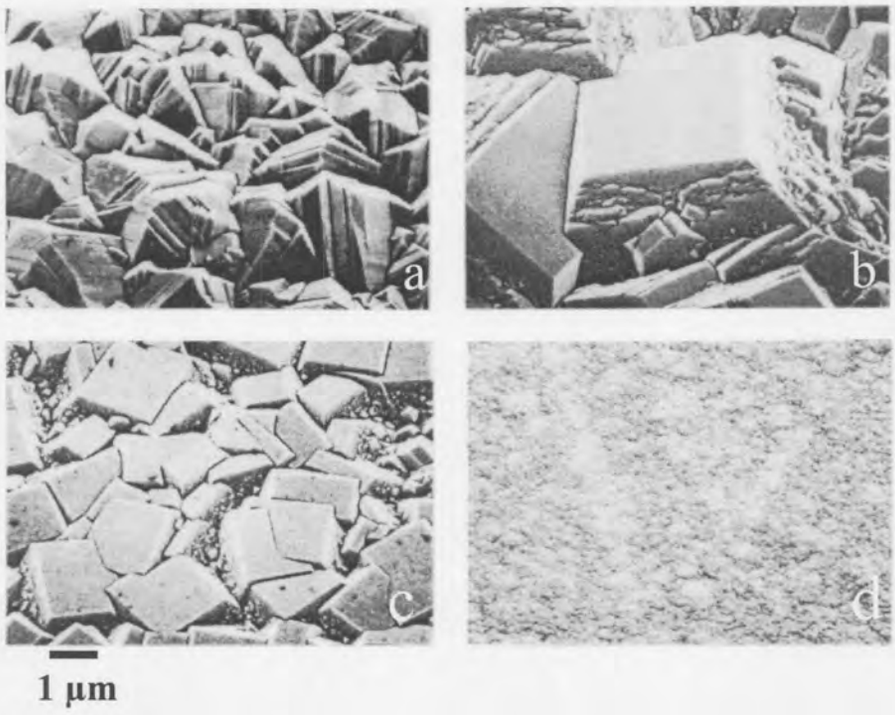

Figure 2.3 : Morphology of as-grown surfaces as the concentration of methane in the feed gas is increased from 0.5% to 5.0%, (a) 0.5%, (b) 2%, (c) 4%, (d) 5% [9]

Figure 2.4 represents the fractured cross-sections of as-grown films grown at methane concentrations of 0.5 – 5.0%. The texture of the films deposited at methane concentrations of 0.5 – 4.0% seems to be columnar or better described as diamond 'whiskers'. Sato and Kamo also found that the growth rate increased with increasing methane concentration. However, a methane concentration of approximately 5.0% or more resulted in the production of inferior quality diamond films. This was evidenced by the reduction of the diamond peak (1332 cm^{-1}) and the occurrence of a broad non-diamond carbon peak (approx. 1550 cm^{-1}) in the Raman spectrum.

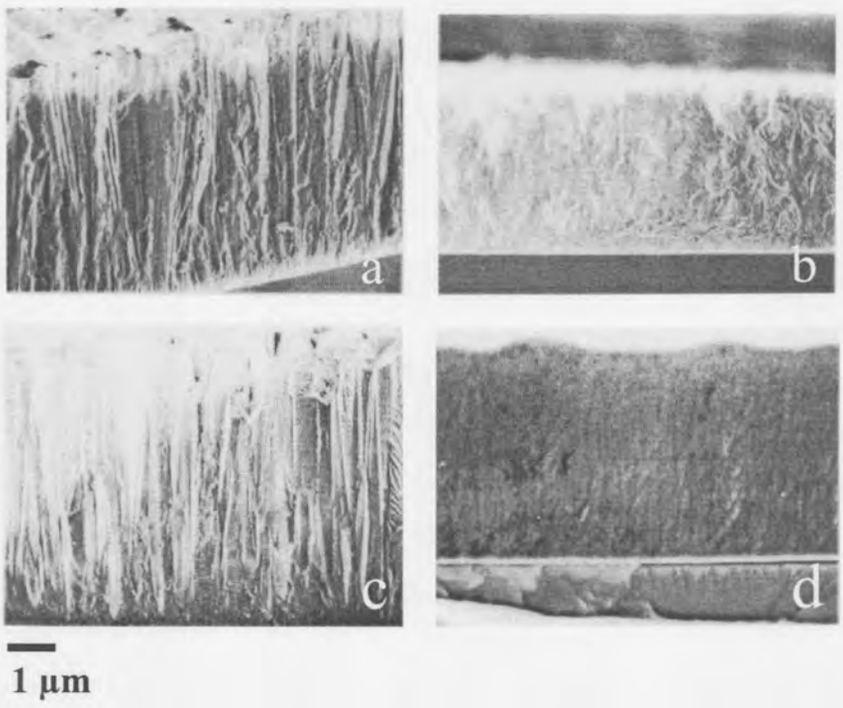

Figure 2.4 : Fractured cross-sections of as-grown films grown at methane concentrations of 0.5 – 5.0%, (a) 0.5%, (b) 2%, (c) 4%, (d) 5% [9]

According to the work undertaken by Hussain et. al. [10], the quality of the diamond thin film was found to be further dependent on the system pressure and the substrate temperature. It was found that, as the reaction chamber pressure decreased from 60 torr to 5 torr, the nucleation density of the diamond crystals on the substrate surface increased. This reduced the crystal size of the diamond film and increased the film coverage. Furthermore, the substrate temperature was found to play a very important role in determining the diamond crystal size. As the substrate temperature decreased from 920°C to 860°C, the crystal size of the diamond film also decreased.

Figure 2.5 illustrates the dependence of the morphology of the diamond film on the methane concentration and the substrate temperature. The growth conditions may be divided into regions A-F : in region A, no or little deposition of either diamond or graphite takes place; in B, the (111) face predominates; in C, (111) and (100) faces occur with comparable frequency; in D, (100) predominates; in D*, the (100) face predominates and diamond grains grow preferentially along the <100> axis; and in E, the surface is smooth and the crystalline morphology is lost. As the methane concentration or substrate temperature increases, the content of diamond in the CVD film decreases.

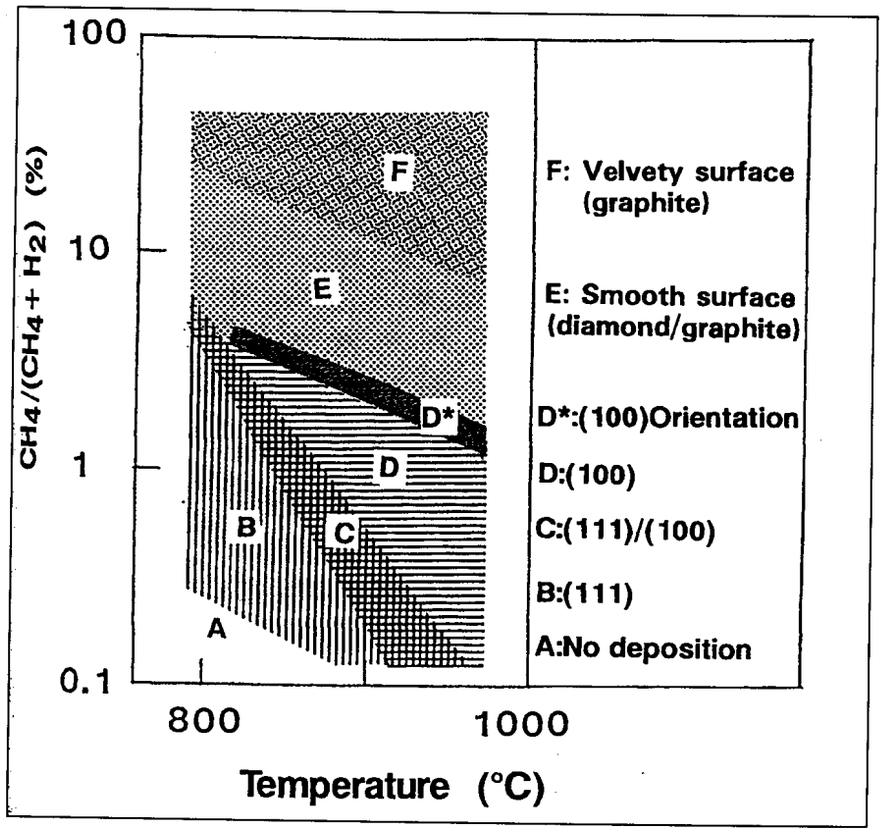

Figure 2.5 : Diagram illustrating the dependence of the morphology of the diamond film on the methane concentration and the substrate temperature [9]

2.4 Effect of boron on CVD diamond

Diamond is a wide band gap semiconductor and its bonding orbitals (valence band) are filled, while its anti-bonding orbitals (conduction band) are much higher in energy. The energy gap is therefore too great for diamond to be conductive or for diamond to absorb visible light. Therefore pure diamond is termed an insulator and appears colourless. However, the presence of trace amounts of boron in diamond leads to a blue colouration. It appears that the more boron present in the diamond, the deeper the blue colour observed.

Carbon contains four valence electrons, whilst boron contains only three valence electrons. When the diamond lattice is doped with boron, the boron atom substitutes a carbon atom in the crystal lattice, thereby forming a B-C bond. Since boron contains only three valence electrons, one of the B-C bonds must be deficient by one electron. Using band theory [11], it is found that the energy level associated with each single-electron B-C bond does not form part of the valence band of diamond. Instead, it forms a discreet level or atomic orbital just above the top of the valence band (refer to **Figure 2.6** [12]). This level is known as an acceptor level because it is capable of accepting an electron, thereby creating a positive hole in the valence band.

Positive holes move when an electron enters them, leaving its own position vacant as a fresh positive hole. This transfer of charge under an applied potential is what makes boron-doped diamond conductive.

In addition, the relatively small gap (0.1 eV) between the valence band and this acceptor level means that the electrons situated at various energy levels in the valence band, may be excited into the acceptor level by light in the lower energy wavelengths of the visible spectrum, so that mostly red, but also some orange, yellow and green light is absorbed. Blue light is not absorbed and that is the colour that is observed.

The investigation carried out by Kanda et. al. [4] entailed a detailed study based on the uptake of nitrogen and boron in the various growth sectors : (111), (001), (011) and (113). Denoting the concentrations of nitrogen atoms by N_D, it was found that N_D (111) > N_D (001) > N_D (113) > N_D (011).

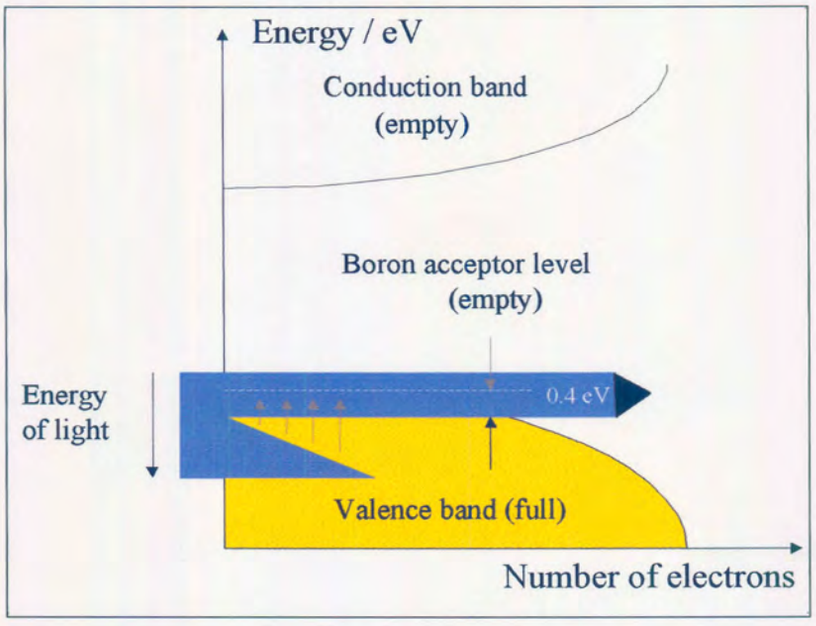

Figure 2.6 : Energy level diagram for boron [11]

The semiconducting property of diamond depends on the uncompensated boron concentration present in the diamond film. Denoting the total boron concentrations by N_A, the uncompensated boron acceptor concentrations will be $(N_A - N_D)$. **Figure 2.7** illustrates a schematic diagram (Kanda diagram) depicting the behaviour of the relative uncompensated boron acceptor concentrations, $(N_A - N_D)$, in the various growth sectors when moving from low (B_L) to high (B_H) levels of boron doping. It is important to note that semiconducting behaviour begins in each sector as N_A exceeds N_D for that sector. For a lightly doped diamond sample, it was found that the uncompensated boron acceptor concentrations for the various facets decreased in the following order: (011) > (113) > (001) > (111), whereas for a more heavily boron doped sample, it decreased as follows: (111) > (011) > (113) > (001).

In a boron-doped CVD diamond film, the specific resistance of diamond depends on the boron content of the film [13]. It can vary from 10^4 Ω.cm (at a content of boron atoms in diamond of approx. $10^{18}cm^{-3}$) to tenth and even thousandth fractions of Ω.cm (at a content of boron atoms in diamond of approx. $10^{21}cm^{-3}$). As the resistivity of the diamond decreases, the diamond acquires successively the properties of a semiconductor, a degenerate semiconductor and then of a semimetal.

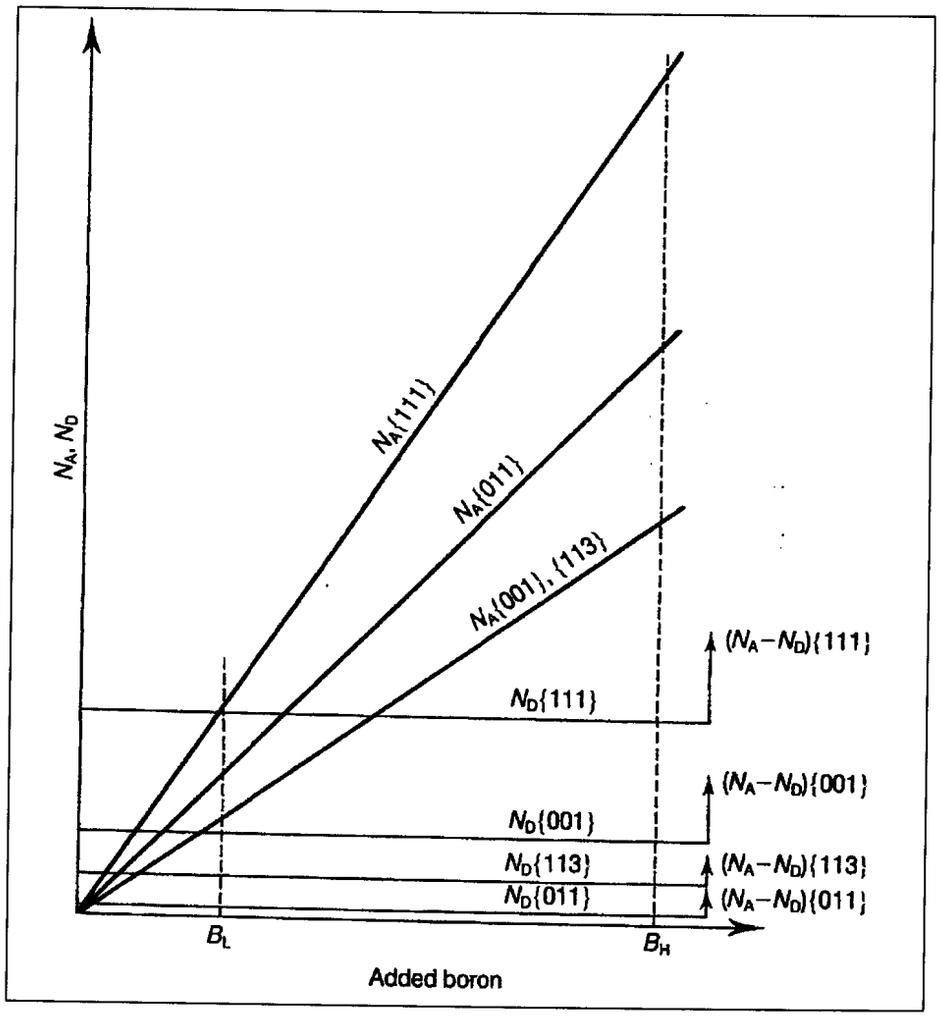

Figure 2.7 : Schematic diagram (Kanda diagram) depicting the behaviour of the relative uncompensated boron acceptor concentrations, ($N_A - N_D$), in the various growth sectors on moving from low (B_L) to high (B_H) levels of boron doping [9]

2.5 References

[1] http://www.chm.bris.ac.uk/pt/diamond/end.htm

[2] X K Zhang, J G Guo and Y F Yao, **Phys. Stat. Sol., (a) 133** (1992) 377.

[3] K Okano, H Naruki, Y Akiba, T Kurosu, M Iida and Y Hirose, **Japanese Journal of Applied Physics, 27** (1988) L173.

[4] K Okada, H Kanda, S Komatsu and S Matsumoto, **Mat. Res. Soc. Symp. Proc., 593** (2000) 459.

[5] K Miyata, K Kumagai, K Nishimura and K Kobashi, **J. Mater. Res., 8** (1993) 2845.

[6] J Xu, M C Granger, Q Chen, J W Strojek, T E Lister and G M Swain, **Analytical Chemistry News & Features, 69** (1997) 591A.

[7] H B Martin, A Argoitia, U Landau, A B Anderson and J C Angus, **J. Electrochem. Soc., 143** (1996) L133.

[8] P Chen and R L McCreery, **Anal. Chem., 68** (1996) 3958.

[9] J E Field, **The Properties of Natural and Synthetic Diamond,** Academic Press Limited (1992) 429.

[10] A Hussain, D Zhou, L Chow and V Desai, **The Minerals, Metals and Materials Society,** (2000) 141.

[11] A R West, **Solid State Chemistry and its Applications,** John Wiley & Sons Limited (1984) 75.

[12] A Butler and R Nicholson, **Chemistry in Britian,** (1998) 34.

[13] Y V Pleskov, **Russian Chemical Reviews, 68** (1999) 381.

CHAPTER 3

Surface structure and chemistry of diamond and boron-doped CVD diamond

3.1 Surface structure and chemistry of diamond

Naturally occurring diamonds are found in two types of deposits, namely alluvial and kimberlite deposits [1]. There is a tendency for the alluvial diamonds to be predominantly hydrophilic and those from a kimberlite pipe to be hydrophobic. Separation techniques for these two types of diamonds were thus developed based on their respective surface chemical properties [2]. Using grease tables or flotation techniques [1], it was found that hydrophobic diamonds readily adhered to the grease, whereas hydrophilic diamonds did not.

The reason why some diamonds were hydrophobic and others hydrophilic was initially not well understood. It was believed that the hydrophilic properties of the alluvial diamonds arose as a result of the adsorption of inorganic salts such as sodium chloride and ferric oxides onto the surface of the diamond [1]. After extensive research, it was found that hydrophobic diamonds became hydrophilic on exposure to water [1,2], which led researchers to believe that diamonds are hydrophilic because of the oxidation and hydration of the diamond surface rather than the adsorption of inorganic salts onto the

surface. This was to ultimately lead to, and inevitably be the foundation for the developing research into the importance of the surface chemistry of diamond.

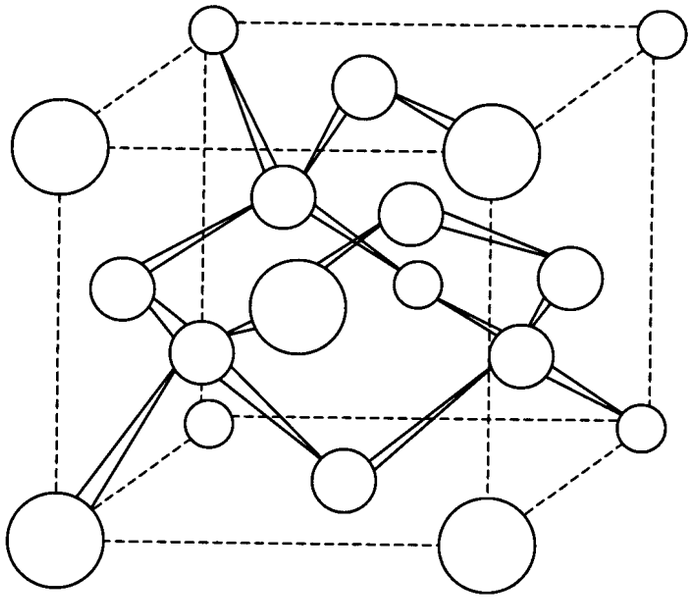

Figure 3.1 : Crystal structure of the diamond lattice [1]

Figure 3.1 represents the crystal structure of a diamond lattice. Each carbon atom is tetrahedrally surrounded by four other carbon atoms. The most frequently occurring facets are the octahedral (111), cubic (100) and rhombic dodecahedral (110) facets [3]. Carbon atoms may be singly bonded on the edges and corners of diamond crystals or anchored with two or three valence bonds to the bulk structure in the (100) and (111) crystal faces (**Figure 3.2**).

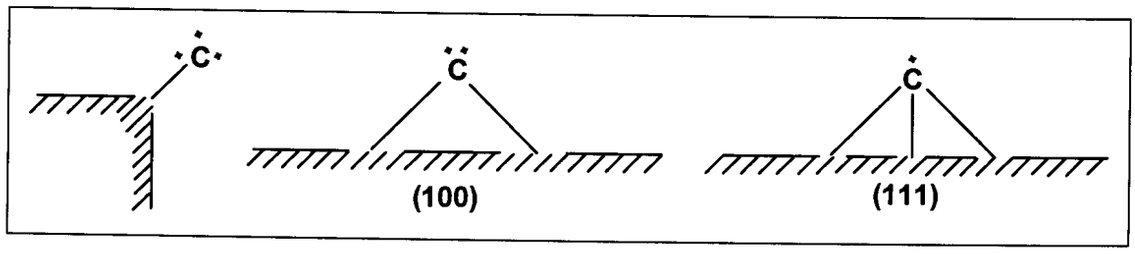

Figure 3.2 : Bonding of carbon atoms to the diamond surface [4]

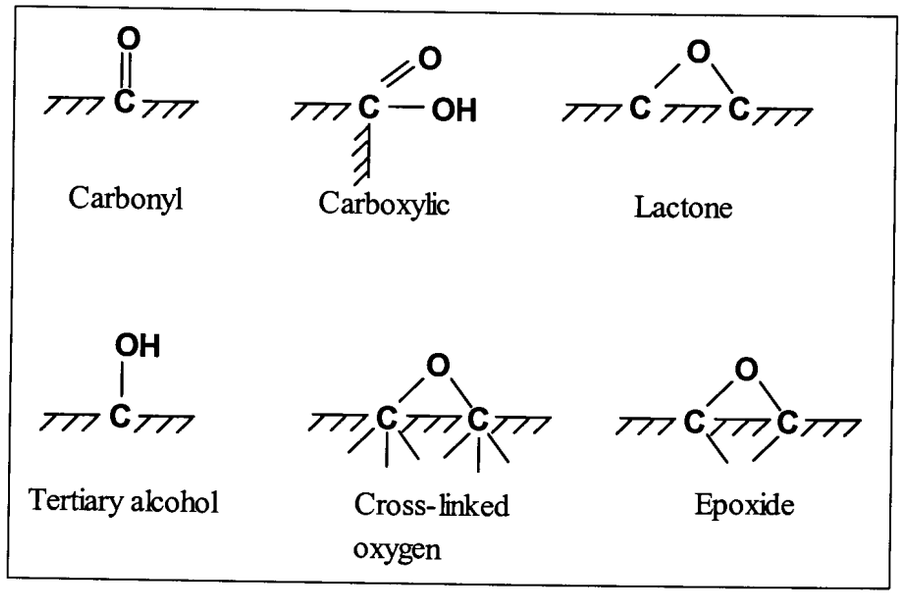

Figure 3.3 : Possible oxygen groups on the diamond surface [2]

Figure 3.3 represents possible oxygen groups on the surface of diamond. Shergold et. al. [2] found that less than 10% of surface carbon atoms are involved in acidic and carbonyl groups. According to the classification of Boehm [4], about 55% of the acidic and carbonyl groups are carboxylic and lactonic in nature and the rest alcohol and carbonyl groups. These carboxylic and lactonic groups are probably found on the edges of the diamond surface rather than on a flat diamond surface because both groups involve a carbon atom with only one bond linking it to another carbon atom within the solid. **Table**

3.1 illustrates the surface groups possibly arising from the saturation of the free valences of carbon with oxygen and hydrogen.

Table 3.1 : Surface groups possibly arising from the saturation of the free valences of carbon with oxygen and hydrogen [3]

Facet	Free valence electrons on carbon	Oxygen group	Hydrogen group
(111) or (110)	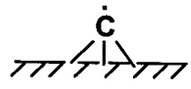	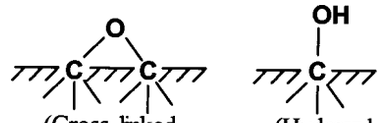 (Cross-linked oxygen) (Hydroxyl group)	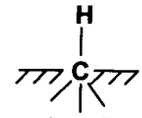 (tert. C-H group)
(100)		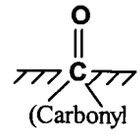 (Carbonyl group)	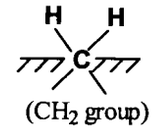 (CH_2 group)
Edges and Corners	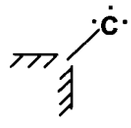	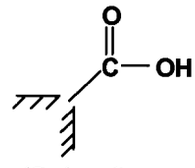 (Carboxylic group)	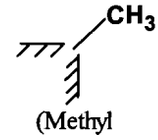 (Methyl group)

Gordeev and Smirnov [5] investigated the effect of the various functional groups synthesised on the surface of synthetic diamond submicron powders on their respective water vapour adsorption isotherms. Chloride, hydride, methyl and hydroxyl functional groups were used in the experiment. They found that the preparations containing a large number of strongly hydrophilic centres (hydroxyl or carbonyl functional groups)

adsorbed far more water than did the other diamond preparations. The activities of the functional groups were ranked according to their decreasing adsorptivity towards water vapour : OH > COOH > Cl > CH_3 > H. Since the activity is related to the polarity of the surface groupings, this implies that the hydroxyl group is much more polar than the methyl or hydride groups. The above ranking agrees with the fact that the adsorption of polar water molecules takes place preferentially on the surface centres that have a high dipole moment (**Table 3.2**) and are also capable of forming hydrogen bonds with the adsorbate.

Table 3.2 : Dipole moment of functional groups [6]

Functional group	Dipole moment, μ
-OH	1.51
-COOH	-
-Cl	1.47
$-CH_3$	0.4
-H	0.4

3.2 Surface structure and chemistry of boron-doped CVD diamond

Chemical vapour deposited diamond is polycrystalline in nature. Depending on the growth conditions, the crystalline structure of CVD diamond could consist predominantly of (111) facets, (100) facets or a mixture of randomly oriented facets. The growth and

surface structure of CVD diamond is best described using the Van der Drift model (**Figure 3.5**). CVD diamond is usually deposited on silicon or tungsten substrates. According to the model, the initial layer of CVD diamond consists of randomly oriented octahedral, cubic and rhombic dodecahedral facets. The facet which grows the fastest will become predominant. This will result in the CVD diamond film consisting of acicular crystallites. The specific conditions for CVD diamond will determine which facet becomes predominating.

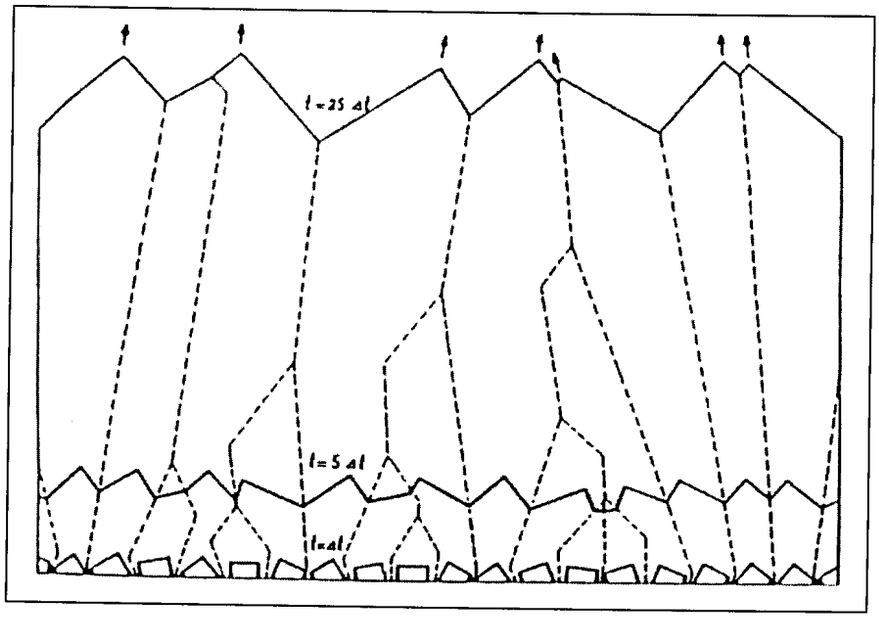

Figure 3.5 : Van der Drift model [7]

Since boron-doped CVD diamond consists primarily of sp^3 carbon covalently bonded in the polycrystalline lattice, it can be assumed that the surface chemistry of boron-doped CVD diamond is analogous to that of natural or synthetic diamond. Since CVD diamond also possesses the three most frequently occurring facets (i.e. (111), (110) and (100)), it is

presumed that similar oxygen functional groups will occur on the boron-doped CVD diamond surface as compared to natural or synthetic diamond (**Table 3.1**).

According to the investigations undertaken by Beamson et. al. [8], hydroxyl, ether, carbonyl and carboxyl functional groups could be identified on organic polymers by their respective peak shifts using X-ray photoelectron spectroscopy (XPS). Using this information and XPS, Goeting et. al. [9] identified the presence of these functional groups on the surface of the boron-doped CVD diamond.

3.3 References

[1] C J Hartley and H L Shergold, **Chemistry and Industry,** (1980) 224.

[2] C J Hartley and H L Shergold, **International Journal of Mineral Processing, 9** (1982) 219.

[3] H P Boehm, **Kolloid Zeitschrift & Zeitschrift fuer Polymere, 227** (1968) 17.

[4] H P Boehm, **Adv. Catalysis, 16** (1966) 219.

[5] S K Gordeev and E P Smirnov, **Kolloidnyi Zhurnal, 44** (1992) 554.

[6] A J Gordon and R A Ford, **The Chemist's Companion,** Wiley, New York (1972).

[7] A Van der Drift, **Philips Res. Rep., 22** (1967) 267.

[8] G Beamson and D Briggs, **High Resolution XPS of Organic Polymers,** Wiley, Chichester, UK (1992).

[9] C H Goeting, F Marken, A Gutierrez-Sosa, R G Compton and J S Foord, **New Diamond and Frontier Carbon Technology, 9** (1999) 207.

CHAPTER 4

Characterisation of boron-doped CVD diamond

4.1 Introduction

There exist various analytical techniques that can provide information on the surface structure as well as on the surface chemistry of solid materials. The information that is gained by using these analytical techniques is invaluable in understanding the characteristics and behaviour of these solid materials. One of the frequently used techniques is scanning electron microscopy (SEM). Unlike ordinary microscopes, the SEM allows for magnifications up to approximately 100 000x to be easily reached, thereby enabling the structures of, for example nano sized particles to be easily obtained.

Another well used technique is X-ray photoelectron spectroscopy (XPS). This is a surface technique that permits the identification of elements on solid surfaces. Another effective technique is Auger electron spectroscopy (AES). XPS and AES are the two major surface analytical techniques and are largely complementary. XPS is more sensitive and gives more useful chemical information, whilst AES has the advantages of greater speed and the potential for high spatial resolution.

Secondary ion mass spectrometry (SIMS) is a technique well known for its high-sensitivity elemental analysis. Laser ablation inductively coupled plasma mass spectrometry (LA-ICP-MS) is less sensitive compared to SIMS, but can readily be applied to solid samples.

The techniques used to analyse the as-received CVD samples were SEM, LA-ICP-MS, Raman and XPS. Contact angle and resistance measurements of the samples were also performed in order to determine the surface state as well as the conductivity of the samples respectively.

4.2 Scanning electron microscopy (SEM)

4.2.1 Theory

Scanning electron microscopy involves the interaction of a beam of primary electrons (produced by an electron gun) with the material being examined. When the primary electron beam strikes the sample, three types of emissions occur, namely secondary electrons, backscattered electrons and X-rays (**Figure 4.1**). These emissions emanate either from the surface of the sample or within the sample.

The secondary electrons are emitted from the surface of the sample and are used to determine the sample topography. Backscattered electrons are emitted from deeper within the specimen, and these electrons provide information related to the atomic number of the specimen. Finally, the emitted X-rays can be used in conjunction with an X-ray detector

to determine which elements are present in the sample. This technique of X-ray emission is called energy dispersive spectroscopy (EDS).

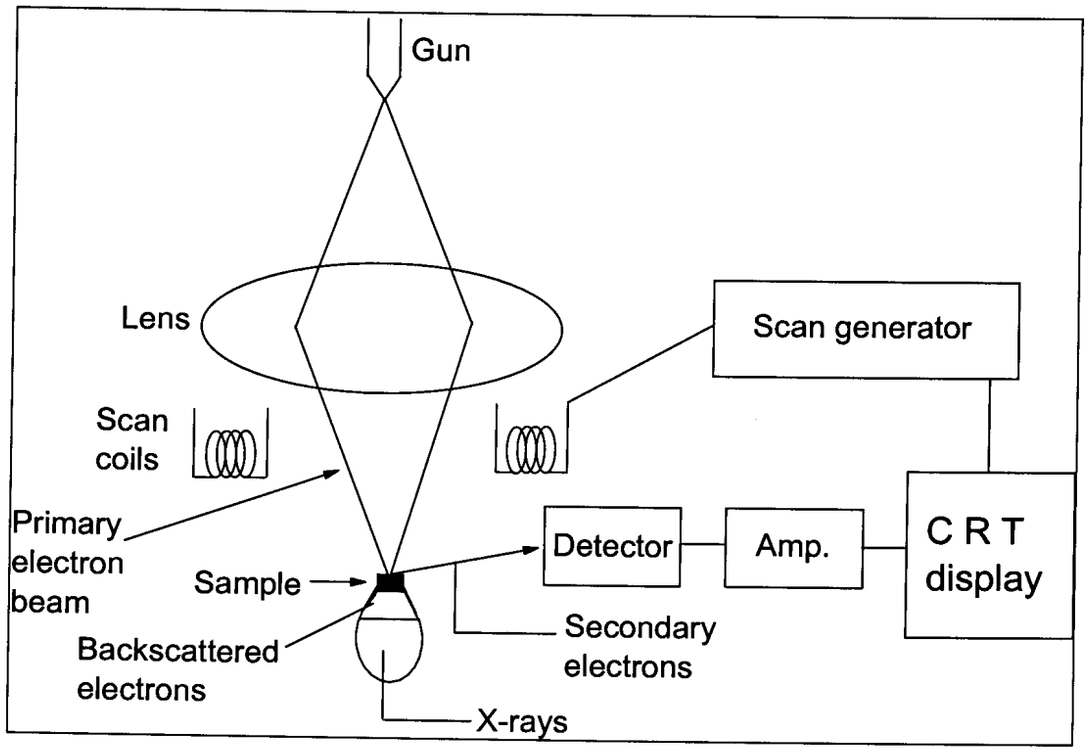

Figure 4.1 : Schematic of the scanning electron microscope (SEM) (modified extract from [1])

During the imaging of a sample, the electron beam scans across the surface of the sample in a raster type pattern. Since the secondary electron detector is connected to the display monitor, as the primary electron beam is scanned across the surface of the sample, the image is shown on the monitor instantaneously. The image formed is based on the intensity of the secondary electrons emitted from the specimen.

In order to obtain a good quality image, the specimen under investigation must be electrically conductive. Otherwise, there will be a build-up of electrons in and around the sample, and this will result in the primary electron beam being repelled from the sample, thereby producing a "poor" quality image.

Various boron-doped diamond samples were analysed using the SEM. Diamond, in the absence of a satisfactory dopant, is rendered non-conductive. One of the techniques adopted to make non-conductive specimens conductive is gold plating of the sample surface. Since the boron-doped diamond samples were conductive due to the presence of boron, gold plating of the surface of the CVD sample was not essential.

4.2.2 Experimental

A Philips ESEM XL 30 was used to analyse the surfaces of six boron-doped CVD diamond samples, obtained from De Beers. The dimensions of each sample were: length = 1 cm, width = 1 cm and thickness = 0.07 cm. CVD samples were initially ultrasonically cleaned with water and acetone before analysis. The boron-doped samples were mounted onto stainless steel stubs using graphite tape and then inserted into the SEM sample chamber. After the chamber was evacuated, the electron beam was focused onto the sample surface and the desired magnification attained. The image was then acquired electronically.

4.2.3 Results and discussion

CVD samples of varying boron content were characterised using the SEM. The manufacturer's estimated boron content of the samples is given in **Table 4.1**. CVDBD6 is the highest boron-doped sample, whereas CVDBD2 is the lowest boron-doped sample. CVDBD1 is undoped. The SEM images of the various boron-doped samples are shown in **Figures 4.2 – 4.7**. From these images, it can be seen that the CVD samples consist of randomly oriented facets.

Table 4.1 : Estimated boron concentrations of CVD samples

Sample	[B] / mg/L	[B] / atoms.cm^{-3}
CVDBD1	0	0
CVDBD2	76	1.50×10^{19}
CVDBD3	438	8.64×10^{19}
CVDBD4	799	1.58×10^{20}
CVDBD5	1160	2.29×10^{20}
CVDBD6	1521	3.00×10^{20}

Numerous grain boundaries are also present. This observation is important from a sample homogeneity point of view, as it is known that impurities concentrate at grain boundaries [2]. The undoped and medium boron-doped samples were found to be similar in terms of their crystallite sizes, which were considerably larger than those of the low boron-doped and high boron-doped samples. This will impact on the surface area of the samples, with

the medium doped sample expected to have a slightly smaller surface area, and therefore to generate a slightly smaller current when used as an electrode, than the other samples. One way of ensuring that all the sample surface areas are the same, is to polish the sample. However, this would alter the surface state in terms of chemical functionalities, and it was therefore decided to work with cleaned but unpolished samples during the voltammetric investigation.

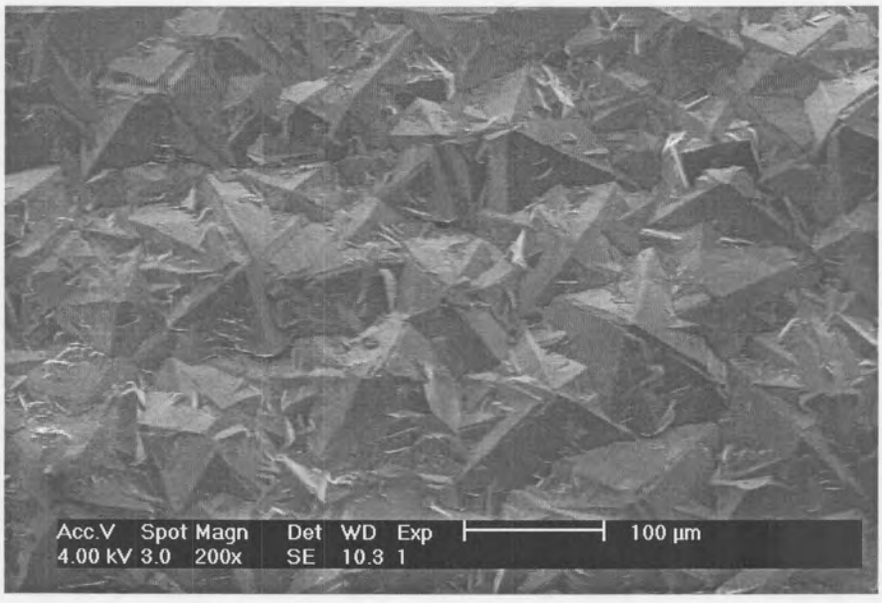

Figure 4.2 : SEM image of undoped CVD diamond

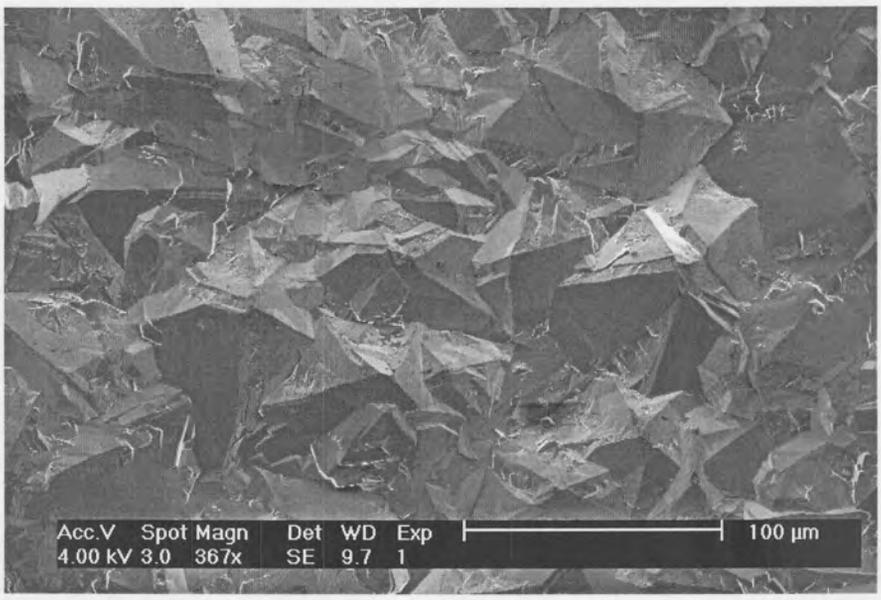

Figure 4.3 : SEM image of low boron-doped CVD diamond (CVDBD2)

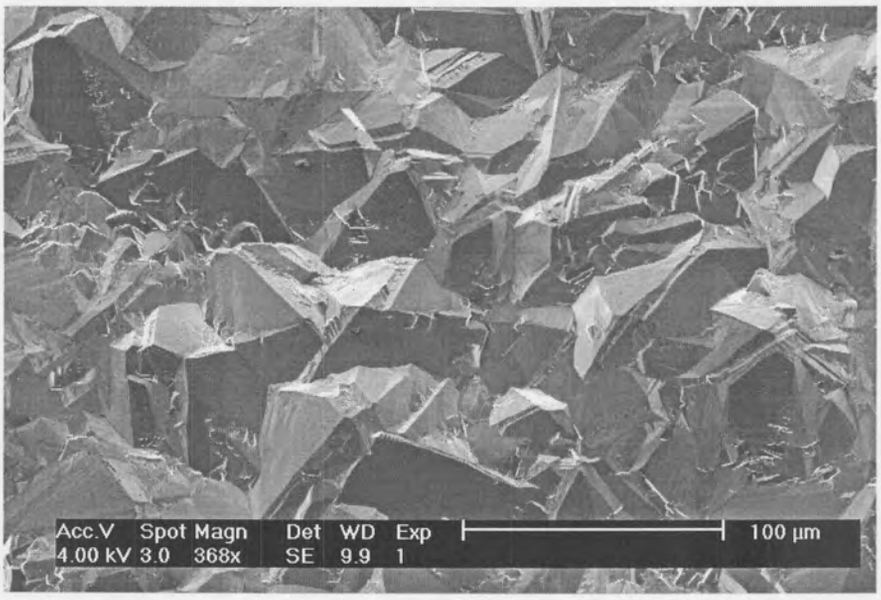

Figure 4.4 : SEM image of low-medium boron-doped CVD diamond (CVDBD3)

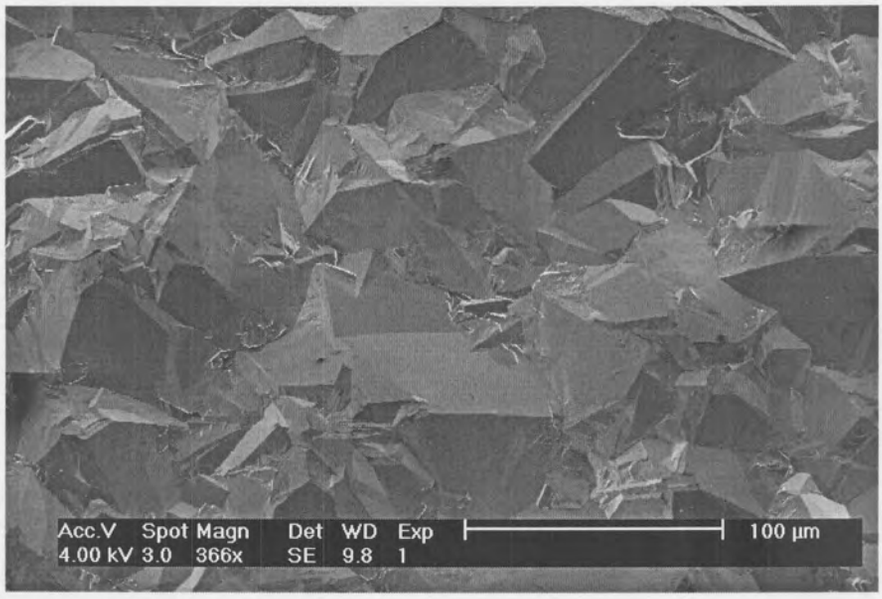

Figure 4.5 : SEM image of medium boron-doped CVD diamond (CVDBD4)

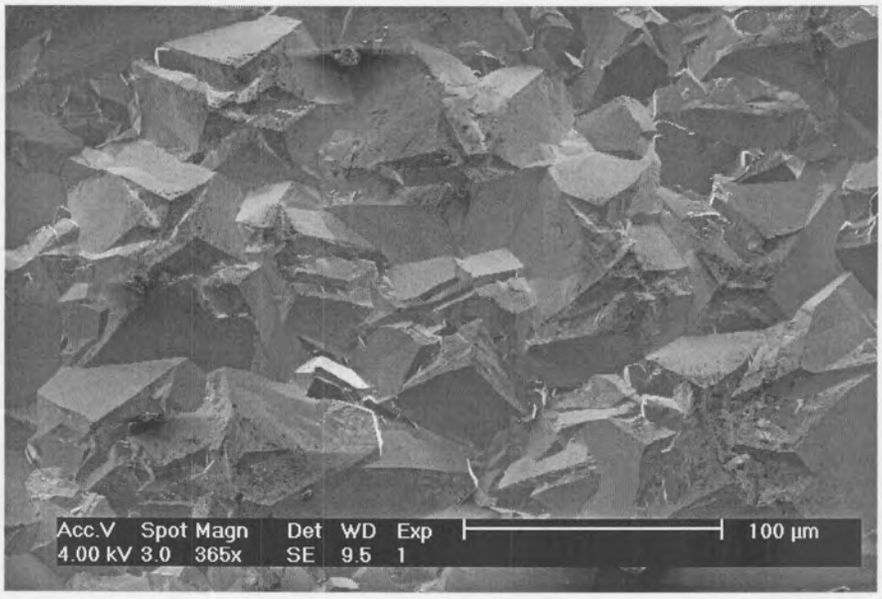

Figure 4.6 : SEM image of medium-high boron-doped CVD diamond (CVDBD5)

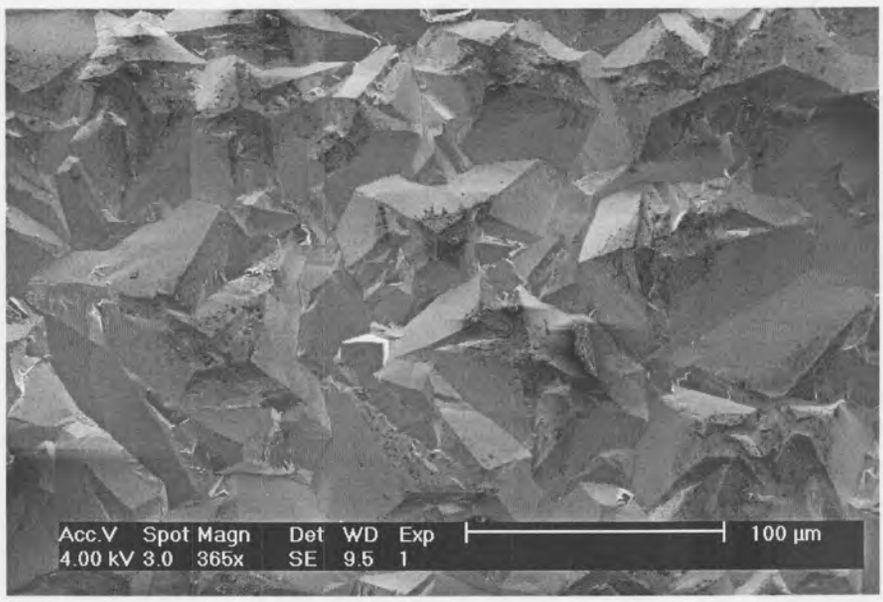

Figure 4.7 : SEM image of high boron-doped CVD diamond (CVDBD6)

4.3 Laser ablation inductively coupled plasma

4.3.1 Theory

The laser ablation ICP-MS is a trace element microprobe which combines the spatial resolution of an ultraviolet laser beam with the mass resolution and elemental sensitivity of an inductively coupled plasma mass spectrometer (ICP-MS). This system is thus suitable for the analysis of boron concentration in the CVD samples. A schematic diagram depicting the laser ablation ICP-MS system is shown in **Figure 4.8**.

The laser beam is generated from a Nd-YAG laser with a wavelength range from 1 micron (infra-red region) to 266 nanometers (ultraviolet region). Samples are located in an enclosed sample cell that is continuously purged with argon gas. The top surface of the

sample cell, which consists of a thin flat plate of quartz or a thin mylar film, is transparent to the laser light and the laser beam can therefore be focused onto the sample surface causing ablation.

Samples may either be mounted as irregular shapes or polished/unpolished thin sections. The physical form of the sample is irrelevant as long as the sample is positioned under the laser beam. Samples are usually viewed through a high-resolution colour video camera. A small volume of material is ablated from the sample surface using the laser beam. The ablated material is then transported in an argon carrier gas directly to the inductively coupled plasma. The resulting ions are then drawn into a quadrupole mass spectrometer for detection. LA-ICP-MS has various advantages and disadvantages [4].

Advantages

- There is no need for chemically dissolving samples, thereby reducing the risk of contamination and sample losses
- Very small samples can be analysed
- The spatial distribution of elements can be determined

Disadvantages

- There is a need for an internal standard to correct for the differences in the ablation rate of the sample and of the standard
- The instrument needs to be routinely calibrated

LA-ICP-MS has several geological applications, which may include analysis of rocks, minerals, glasses, fluid and solid inclusions.

4.3.2 Experimental

The analysis of the boron concentration of the CVD samples using the LA-ICP-MS system (Cetac LSX200, Elan 6000 ICP-MS) was carried out at the De Beers GeoScience Centre. **Table 4.2** illustrates the LA-ICP-MS system configuration. A carbon-based oil was used as a standard in order to calibrate the instrument. Small portions of glass capillary tubes were mounted horizontally in epoxy mounts and the surfaces polished to flatten the top portion of each capillary tube. The standard oil (which was doped with boron) was then syringed into the capillaries and these capillaries were thereafter sealed with tape.

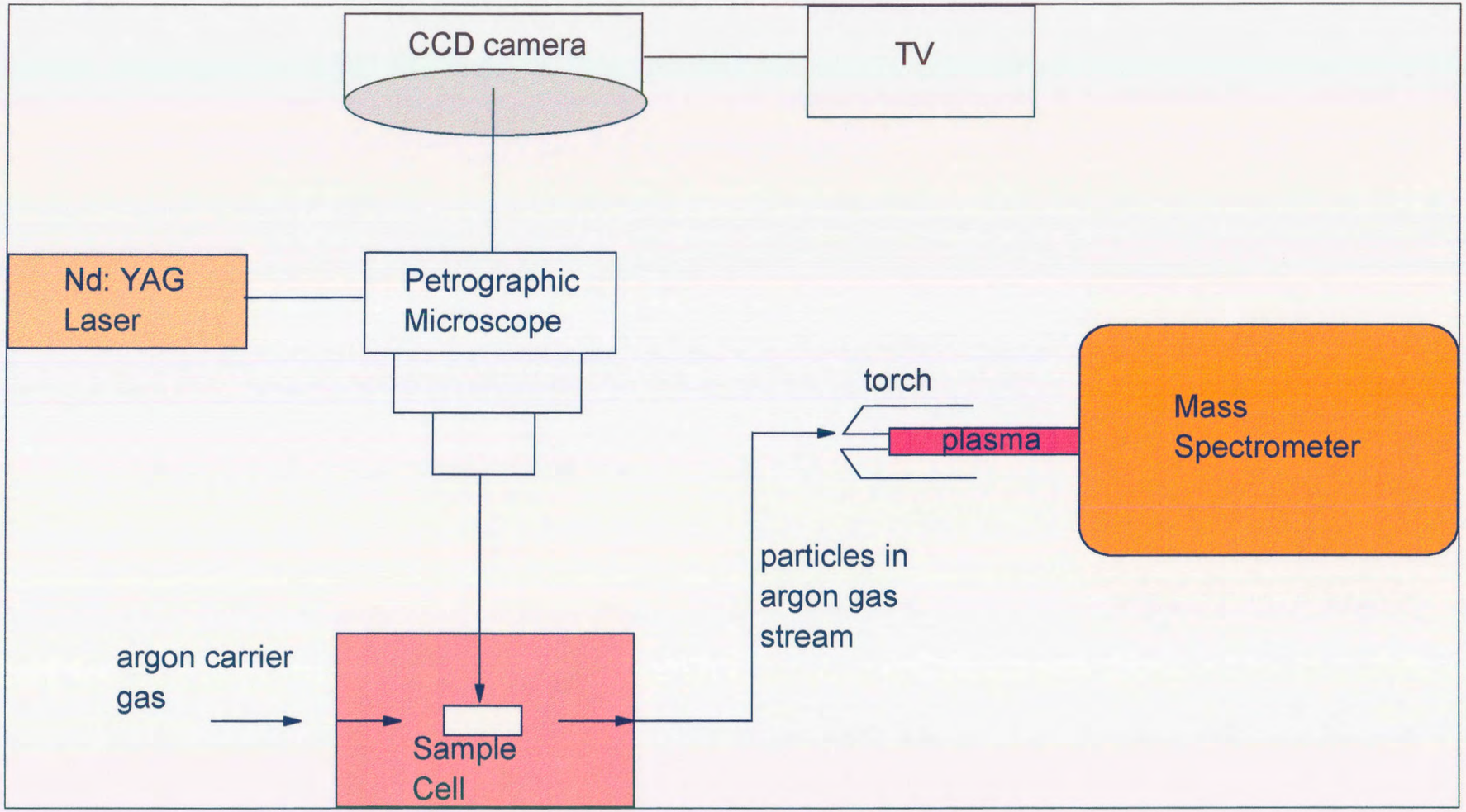

Figure 4.8 : Schematic setup of a LA-ICP-MS unit [3]

Table 4.2 : LA-ICP-MS system configuration

Cetac LSX200	
Laser type :	Q-switched Nd:YAG, frequency quadrupled to 266 nm
Laser energy :	20 mJ
Pulse frequency :	10 Hz
Spot size :	150 micron
Ablation method :	Drill on oil
Elan 6000 ICP-MS	
RF forward power :	1350 V
Carrier gas flow :	1.14 l/min argon and ~1.5 l/min helium
Detector mode :	Peak hopping
Autolens facility :	Activated
Dwell times / sweep :	10 ms per element (except for carbon, 4 ms)
No. of Replicates :	150
Blank acquired for :	30 – 40 s
Ablated sample data acquired for :	10 – 20 s

The carbon in both the oil and the samples was used for internal standardisation to compensate for differential ablation. The carbon concentration of the oil is 86% and that of the diamond films is assumed to be 99.9%. The three samples were ablated using the same laser parameters applied to the standard and quantitative data were obtained.

4.3.3 Results and discussion

Table 4.3 represents the boron concentration results for the three samples analysed. CVDBD1 is the "undoped" sample, CVDBD2 the low boron-doped sample and CVDBD4 the medium boron-doped sample. The estimated boron concentration values were taken from **Table 4.1**. It is seen from **Table 4.3**, that the measured boron concentration values of the CVD samples are very similar to that of the estimated values.

The small amount of boron present in CVDBD1 may be due to boron contamination of the CVD sample during its growth stage. The lower limit of detection for boron with the LA-ICP-MS system was found to be 1 mg/L, and the relative standard deviation for this element ranged from 3.1% to 4.8% for the three pits drilled. **Figure 4.9** illustrates the detailed SEM image of the ablation pit in the glass capillary surface, whilst **Figure 4.10** depicts the SEM image of the diamond thin film surface with two ablation pits.

Table 4.3 : Boron concentrations of CVDBD1, CVDBD2 and CVDBD4

Sample	Measures values		Estimated values
	[B] / mg/L	[B] / atoms.cm^{-3}	[B] / atoms.cm^{-3}
CVDBD1	1.19	2.32×10^{17}	0
CVDBD2	83.8	1.64×10^{19}	1.50×10^{19}
CVDBD4	543	1.06×10^{20}	1.58×10^{20}

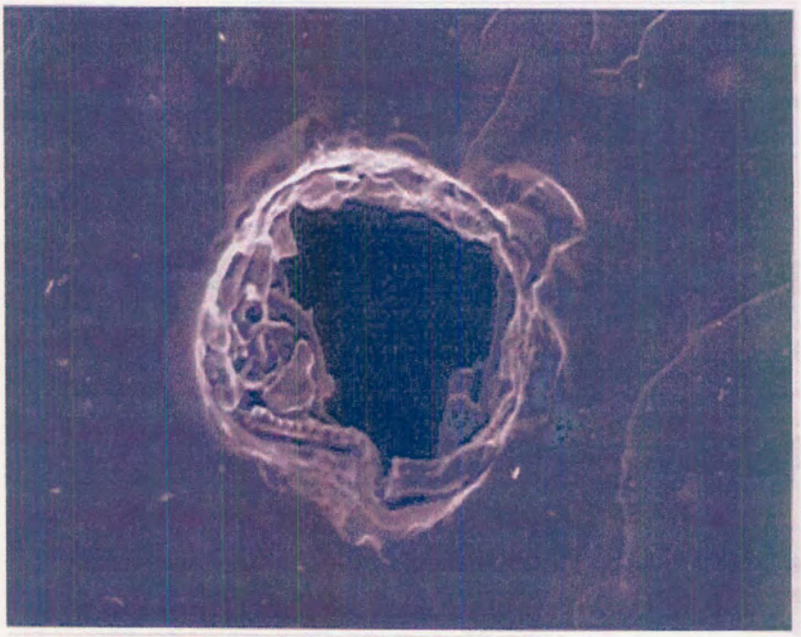

Figure 4.9 : Detailed SEM image of ablation pit in the glass capillary surface

(Magnification ~320x)

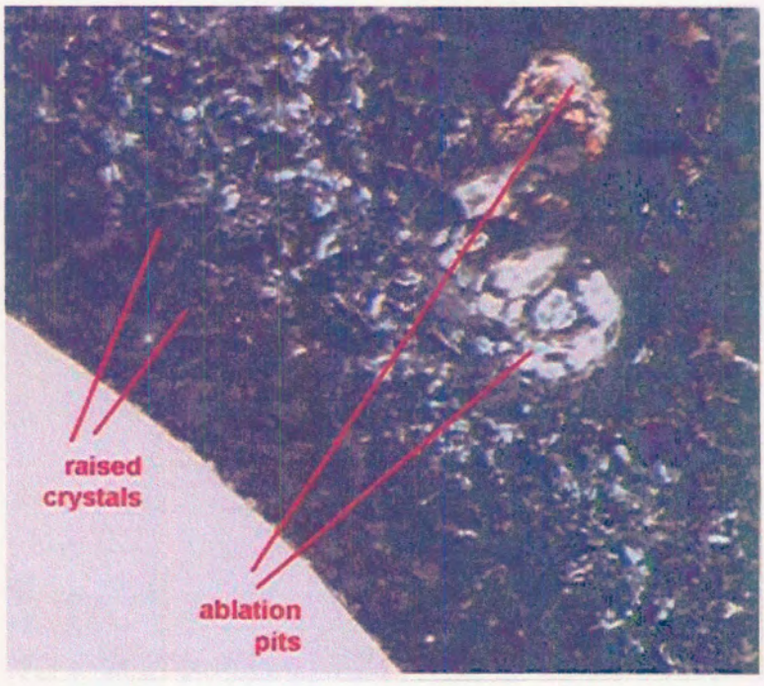

Figure 4.10 : Diamond thin film surface with two ablation pits

An equipment malfunction resulted in decreased sensitivity of the LA-ICP-MS system, so that the boron concentrations of CVDBD3 and CVDBD5 could not be measured. However, the boron concentrations of these samples were estimated using the low, medium and high boron concentration samples (CVDBD2, CVDBD4 and CVDBD6). The boron concentration for all the CVD samples is therefore given in **Table 4.4**.

Table 4.4 : Boron concentrations of CVD samples

Sample	[B] / mg/L	[B] / atoms.cm^{-3}
CVD1	1.19	2.35×10^{17}
CVD2	84	1.64×10^{19}
CVD3	313*	6.18×10^{19} *
CVD4	543	1.06×10^{20}
CVD5	1032*	2.04×10^{20} *
CVD6	1521*	3.00×10^{20} *

*estimated values

4.4 Raman spectroscopy

4.4.1 Theory

The electrochemical behaviour of CVD diamond electrodes can be affected drastically by the presence of sp^2 carbon (graphitic carbon) on the electrode surface. Depending on the growth conditions, sp^2 carbon may be co-deposited with diamond on the substrate surface. It is therefore vital that the extent of graphitisation of the CVD samples be

determined. One of the very few techniques that is extremely useful in distinguishing between the presence of sp^2 carbon and sp^3 carbon in a diamond lattice is Raman spectroscopy. This technique was discovered by an Indian physicist C.V.Raman in 1928 [5]. He was awarded the 1931 Nobel prize in physics for this discovery and his systematic exploration of it.

Raman spectroscopy is a nondestructive method to study the vibrational band structure of materials. It has been extensively used for the characterisation of diamond [6-9], graphite [10] and diamond-like carbon (DLC) [11,12]. This technique can also be applied to the qualitative and semi-quantitative analysis of organic, inorganic and biological systems [5].

A schematic diagram of the Raman spectrometer is given in **Figure 4.11**. The laser is used as the photon source due to its high monochromatic nature. In the visible spectral range, Raman spectrometers use notch filters to cut out the signal from a very narrow range centred on the frequency corresponding to the laser radiation. A microscope is used to focus the laser beam onto the sample. Light from the sample is then passed back through the microscope optics into the spectrometer. Raman shifted radiation is detected with a charge-coupled device (CCD) detector, and a computer is used for data acquisition and curve fitting.

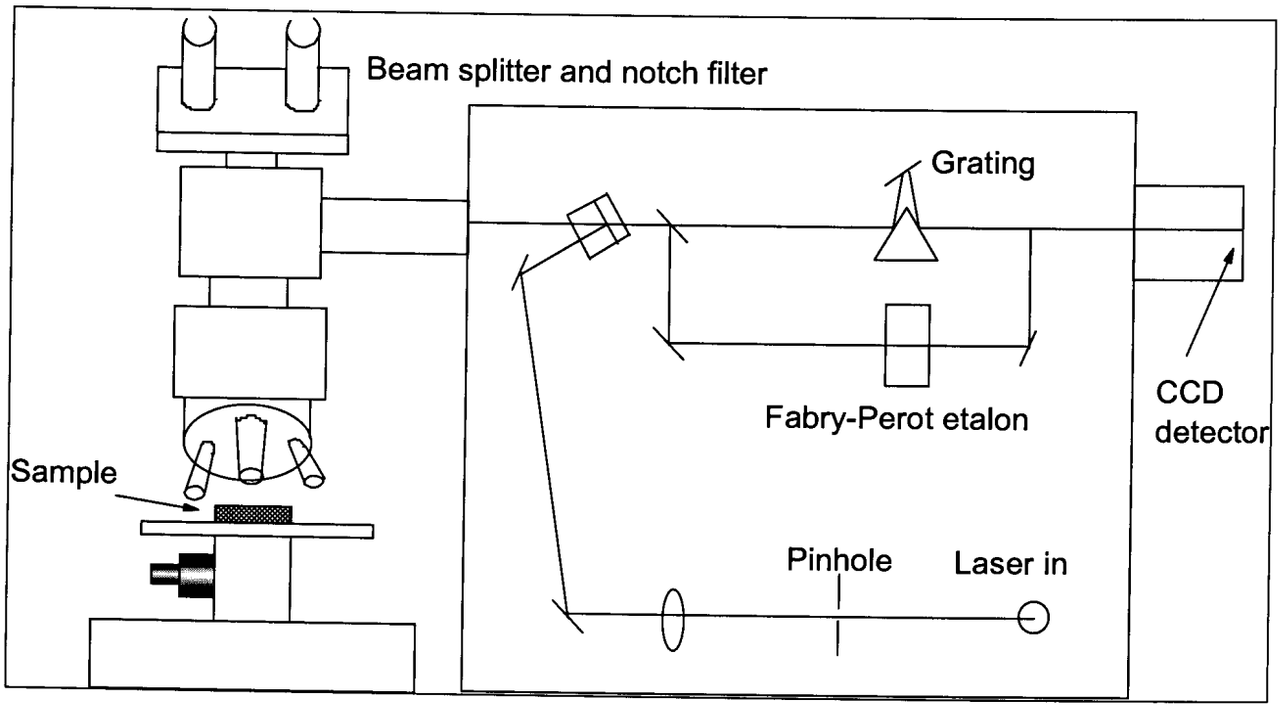

Figure 4.11 : Schematic diagram of a Raman spectrometer [13]

The Raman effect arises when incident light of a particular wavelength excites molecules in the sample, which subsequently scatter the light. While most of this scattered light is at the same wavelength as the incident light (Rayleigh scattering), some of the light is scattered at a different wavelength. This inelastically scattered light is called Raman scatter.

The energy difference between the incident light (E_i) and the Raman scattered light (E_s) is equal to the energy involved in changing the molecule's vibrational state (E_v) (**Equation 4.1**). This energy difference is called the Raman shift.

$$E_v = E_i - E_s \qquad (4.1)$$

Different vibrational or rotational motions of molecules in the sample give rise to different Raman shifted signals being observed. A plot of Raman intensity versus Raman shift is a Raman spectrum.

4.4.2 Experimental

The CVD samples were analysed using a Jobin-Yvon T64000 Raman spectrometer with an Olympus Bx40 microscope attachment. A grating of 1800 grooves/mm was employed to disperse the scattered light onto a liquid nitrogen–cooled CCD detector. The 514.5 nm line of an argon ion laser was used as the excitation radiation for the sample. The Olympus Bx40 microscope attachment with a 100x objective was utilised to focus the argon ion laser to about 3 μm spot size onto the surface of the CVD sample. Spectra for both the rough and smooth surfaces of each sample were recorded.

4.4.3 Results and discussion

Each of the samples had a rough upper surface and a smooth lower surface. Both the rough and the smooth surfaces of the samples were analysed using Raman spectroscopy. **Figure 4.12** denotes the Raman spectra for the rough upper surfaces of the samples. The spectra for CVDBD2 to CVDBD6 are characteristic of high quality diamond films (narrow line width and low background signal).

A very intense one phonon diamond sp^3 carbon peak occurs at a wavelength of approximately 1332 cm^{-1}. This peak is accompanied by a broad flat sp^2 carbon peak occurring at about 1550 cm^{-1}. This non-diamond peak representing the sp^2 carbon impurity phases in the boron-doped samples is clearly observed in the undoped sample and unseen in the boron-doped samples. If the intensity scale of the spectra is expanded, extremely low levels of these impurity phases can be detected. It should be noted that the magnitude of the Raman signal on the ordinate is 50 times more sensitive to the non-diamond carbon form than to the crystalline diamond [14].

Table 4.5 illustrates the sp^2/sp^3 ratio of the rough surface of the CVD samples. This ratio is an average of three sample measurements. From **Figure 4.12** and **Table 4.5**, it may be deduced that the presence of boron in the sample suppresses the formation of sp^2 carbon. However, as the concentration of boron in the sample increases, the ratio of sp^2/sp^3 carbon also increases. This may be due to the decrease of sp^3 carbon as the boron replaces carbon atoms in the diamond lattice, which effectively decreases the Raman cross section for the diamond lattice [15], or it may mean that the boron has improved the quality of the lightest-doped samples by decreasing the content of graphitic and amorphous carbon.

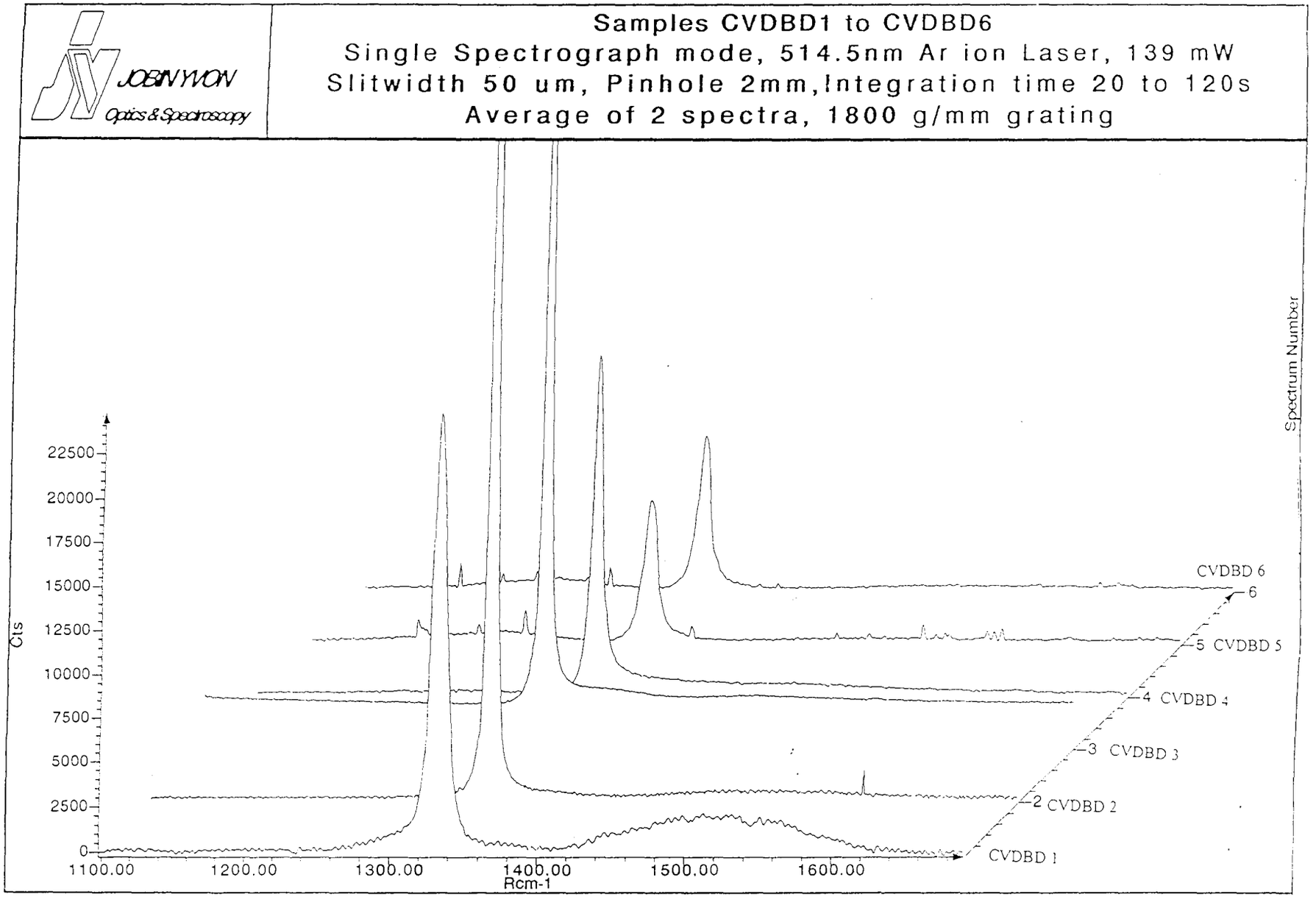

Figure 4.12 : Raman spectra for the rough upper surfaces of the CVD samples

Table 4.5 : Ratio of the sp^2/sp^3 carbon peak areas of the rough surface of the CVD samples

CVD sample	Average sp^2/sp^3 ratio
CVDBD1	2.19
CVDBD2	0.23
CVDBD3	0.71
CVDBD4	1.22
CVDBD5	2.50

Polo et. al. [16] investigated the effect of increasing boron concentration of CVD diamond samples on their respective Raman spectra (**Figure 4.13**). They observed a decrease and a broadening of the diamond peak as the boron concentration increased. The heavily doped sample (75000 mg/L of boron) presents a Raman spectrum with the typical features of amorphous carbon with two broad bands centred around 1350 cm^{-1} and 1570 cm^{-1}.

Figure 4.14 illustrates the Raman spectra for the smooth lower surface of the CVD samples. This surface has a smooth texture due to it being in contact with the substrate (usually silicon or tungsten) during growth. The Raman spectra indicate the strong presence of sp^2 carbon in all the CVD samples. This broad peak occurs at approximately 1550 cm^{-1}.

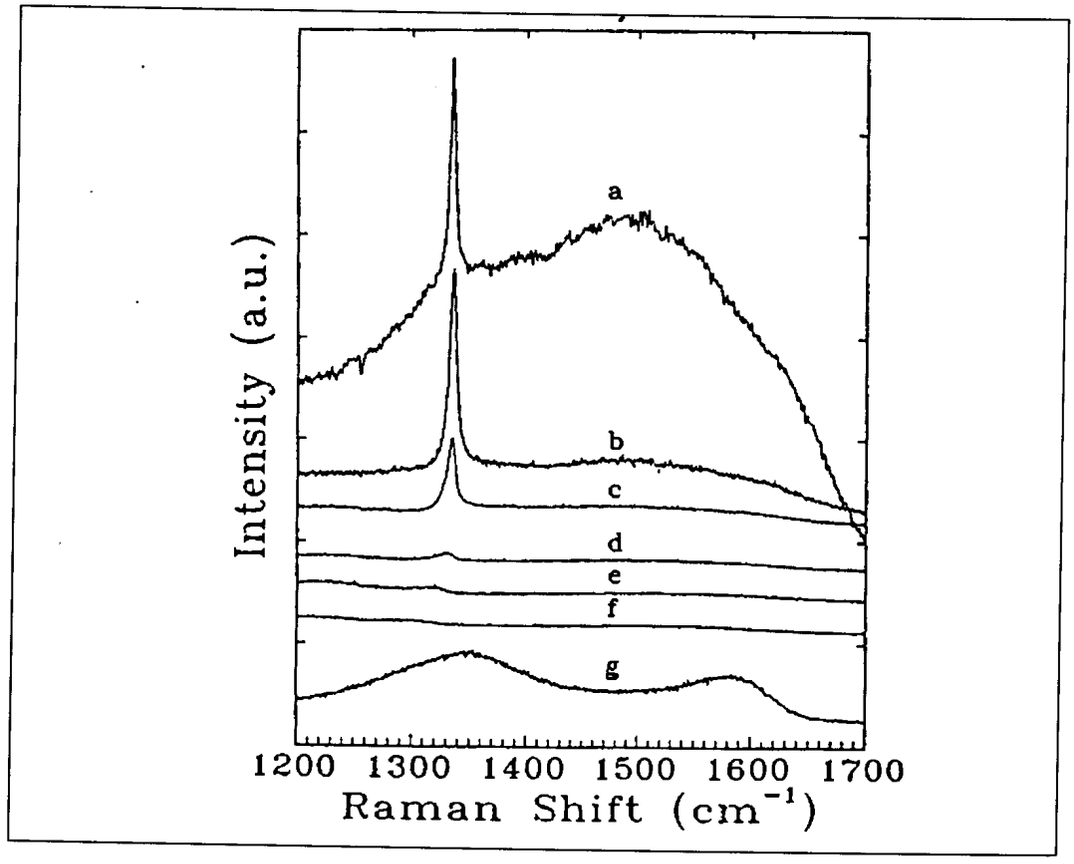

Figure 4.13 : Raman spectra of diamond samples with different boron contents; (a) undoped film, (b) 1333 mg/L B, (c) 2250 mg/L B, (d) 5250 mg/L B, (e) 17500 mg/L B, (f) 2750 mg/L B, (g) 75000 mg/L B [16]

An interesting feature in the spectra illustrated in **Figure 4.14** is that as the boron concentration increases from CVDBD2 to sample CVDBD6, the sp^2 non-diamond peak seems to become more narrow and sharp. This may imply that the graphitic carbon tends to become more crystalline. The smooth lower surface of the CVD samples (i.e. the initial layer deposited during manufacture) was found to contain more sp^2 carbon than the rough upper surface.

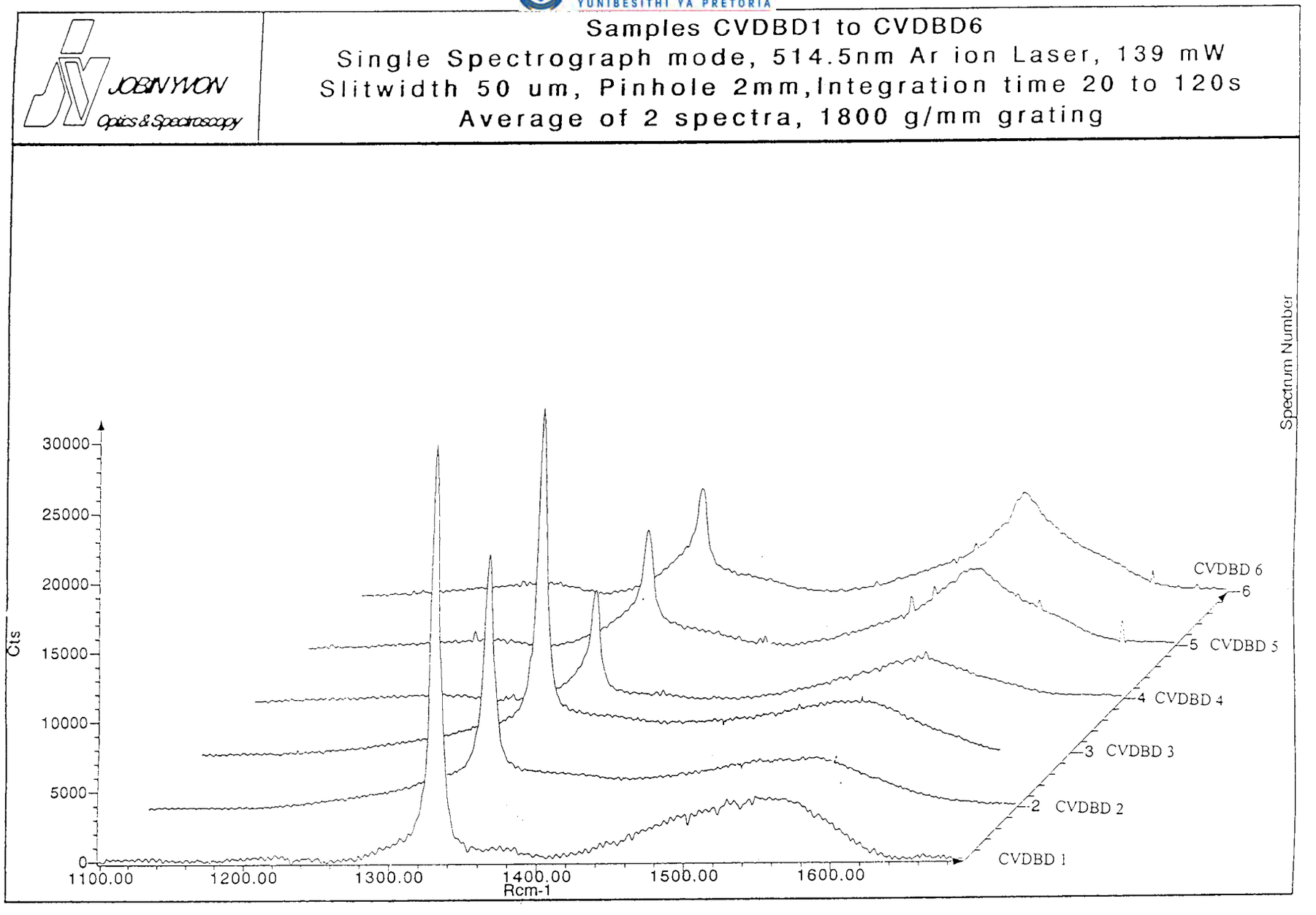

Figure 4.14 : Raman spectra for the smooth lower surface of the CVD samples

4.5 X-ray photoelectron spectroscopy (XPS)

4.5.1 Theory

X-ray photoelectron spectroscopy (XPS, also called electron spectroscopy for chemical analysis, ESCA) was developed in the mid 1960s by K.Siegbahm and his research group [17]. K. Siegbahm was awarded the Nobel Prize in 1981 for his work in XPS. The phenomenon of XPS is based on the photoelectric effect outlined by Einstein in 1905 where the concept of the photon was used to describe the ejection of electrons from a surface when photons impinge upon it. XPS may be used in various areas of application such as polymers, organics, biological specimens, fibres, films, powders and particles [18].

In XPS, the photon is absorbed by an atom in a molecule or solid, leading to ionization and the emission of a core (inner shell) electron [19]. The kinetic energy, E_k, of these emitted photoelectrons is determined by the energy of the X-ray radiation, $h\nu$, and the electron binding energy, E_b, as given in **Equation 4.2** [20].

$$E_k = h\nu - E_b \qquad (4.2)$$

The experimentally measured energies of the photoelectrons are given in **Equation 4.3**, where E_w is the work function of the spectrometer.

$$E_k = h\nu - E_b - E_w \qquad (4.3)$$

Each element yields a characteristic binding energy associated with each core atomic orbital, that is, each element will give rise to a characteristic set of peaks in the photoelectron spectrum at kinetic energies determined by the photon energy and the respective binding energies.

Specific elements in a sample can be identified by the presence of specific peaks occurring at particular energies in the photoelectron spectrum. Furthermore, the intensity of the peaks is related to the concentration of the element within the sampled region. Thus, the XPS technique produces qualitative as well as semi-quantitative information on solid samples. A schematic diagram of the XPS apparatus is found in **Figure 4.15**.

The XPS instrument consists of an X-ray source, an energy analyser for the photoelectrons and an electron detector. In order to analyse and detect the emitted photoelectrons, the sample has to be placed in a high-vacuum chamber. The energy of the photoelectrons is analysed by a spherical analyser, and a channeltron electron detector detects the photoelectrons.

4.5.2 Experimental

A VG Scientific XPS instrument together with VGX 900-W data acquisition and analyzing software were used for the characterisation of the as-received sample, CVDBD4, in terms of its oxygen content. The sample was strapped to a molybdenum sample holder and the holder inserted into the UHV (Ultra High Vacuum) chamber via a

Leybold Heraeus sample introduction rod. The vacuum was then pumped down to 10^{-11} < Pressure < 10^{-10} millibar. Since XPS is a surface analytical technique, the UHV is needed to prevent the atoms in the air from landing on the sample surface and changing its properties.

X-rays from the X-ray source (AlK_{α} radiation) were then focused onto the sample and the resulting photoelectrons emitted. These photoelectrons were then analysed via a channeltron electron detector and an XPS spectrum was produced. The photon energy was 1486.6 eV and the resolution of the spectrometer was 0.1 eV.

4.5.3 Results and discussion

Figure 4.16 represents the XPS spectrum for CVDBD4. The carbon peak occurs at a binding energy of 288 eV and the oxygen peak occurs at a binding energy of 536 eV. For natural diamond, the carbon peak occurs at a binding energy of 284 eV and the oxygen peak occurs at a binding energy of 532 eV. The observed peak shift could be due to the presence of boron on the CVD sample or the oxygen functionalities on the sample.

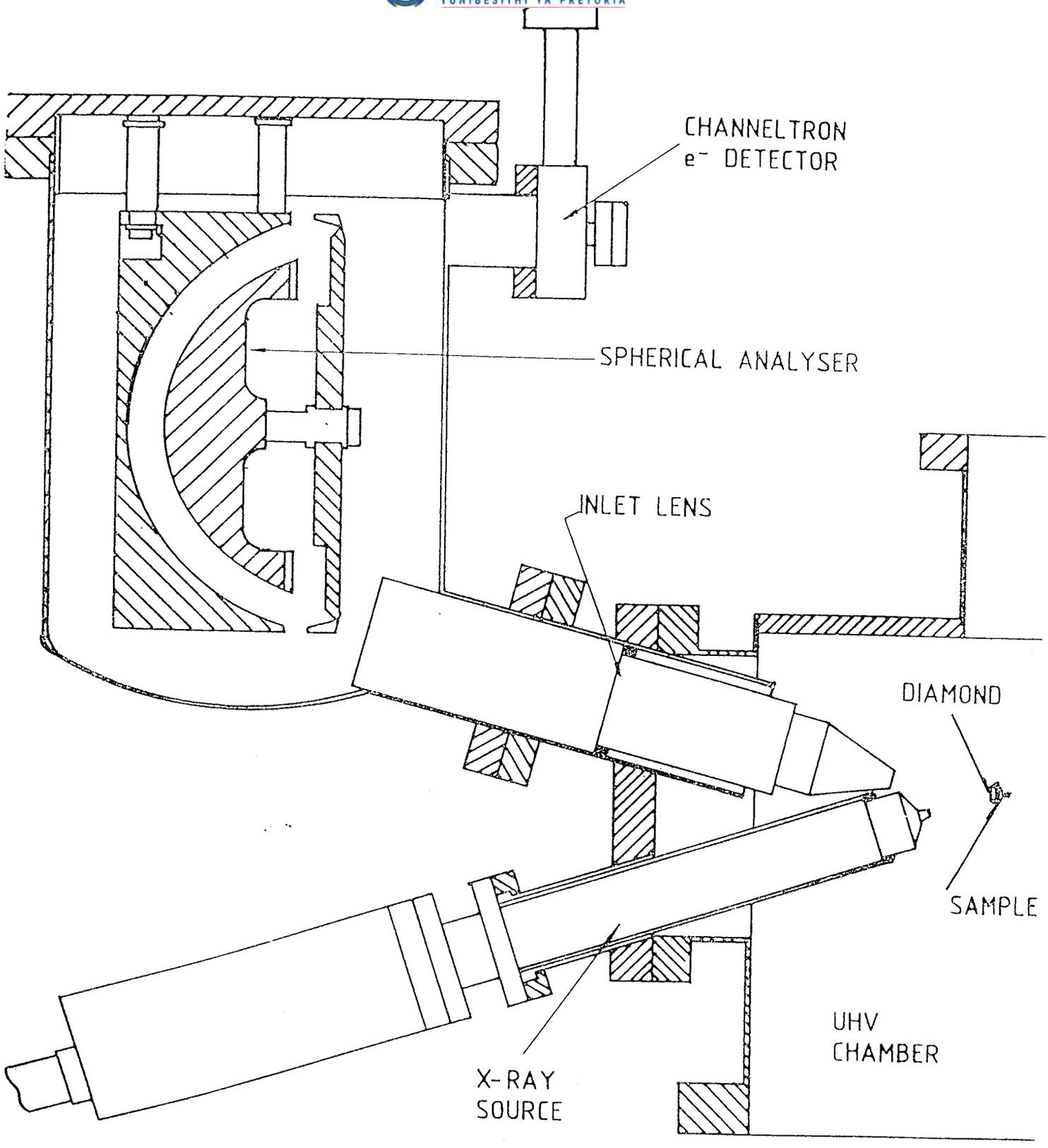

Figure 4.15 : Schematic diagram of the XPS apparatus [21]

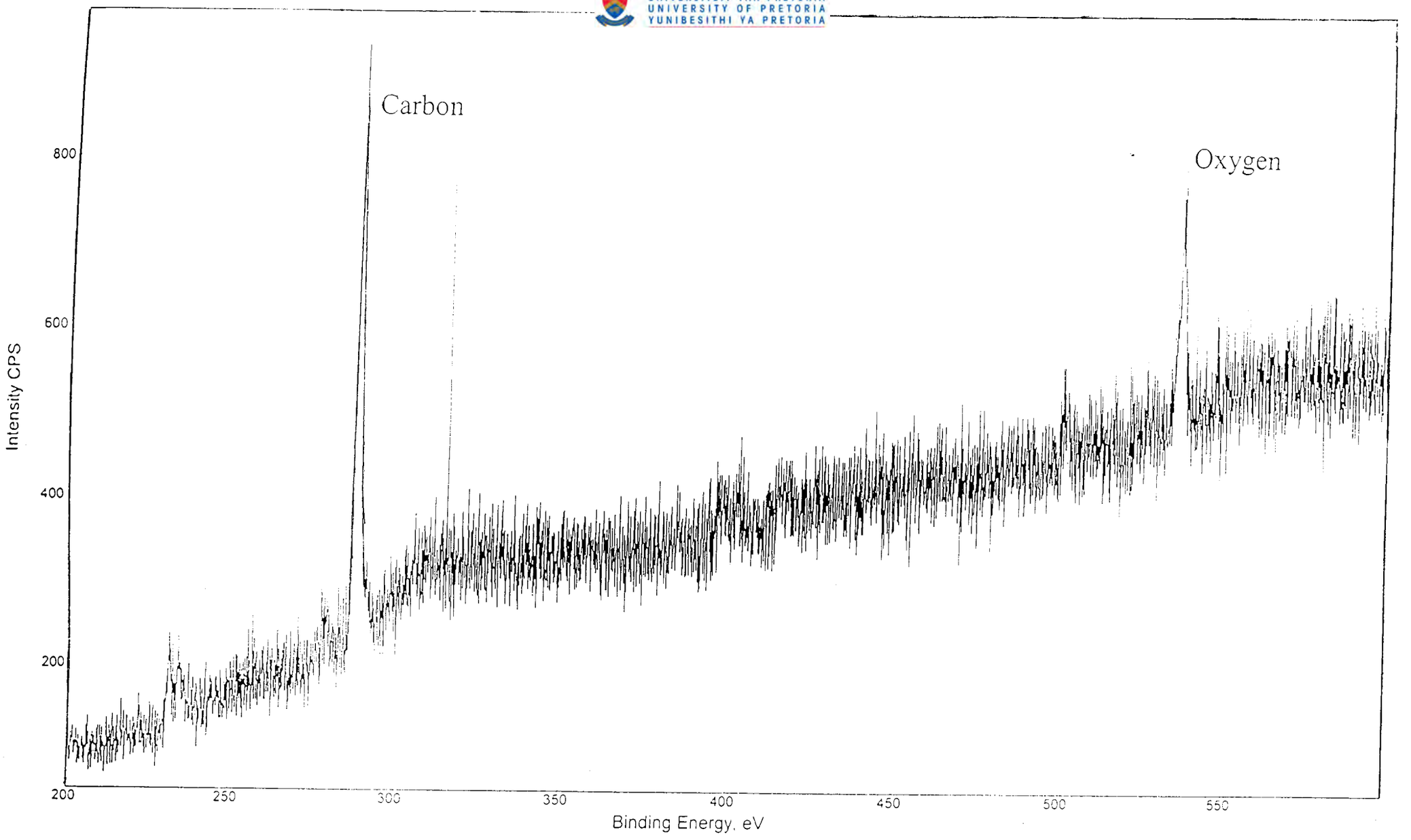

Figure 4.16 : XPS spectrum for CVDBD4

By integrating the peak areas, applying a Gaussian fit to the peaks and using **Equation 4.4**, the oxygen content of the CVD sample was calculated to be 2.37 x 10^{15} atoms/cm^2.

$$\sigma = \frac{Y_m}{Y_s} \times \frac{N \cos\theta\ \mu_s\ \rho_s\ \lambda}{\mu_m\ M_s} \qquad (4.4)$$

Where :

σ = surface oxygen content, atoms/cm^2

Y_m = integrated XPS peak area for adsorbed oxygen atoms corrected for the increase in analyser sensitivity with decreasing kinetic energy

Y_s = integrated peak area for substrate carbon

N = Avogadro's number, 6.023 x 10^{23} atoms/mole

θ = system geometrical constant, 25°

μ_s = photoionization cross-section for carbon, 1.0

μ_m = photoionization cross-section for oxygen, 2.92

ρ_s = diamond density, 3.51 g/cm^3

λ = photoelectron escape depth (AlK_α)

M_s = mass number of carbon, 12.01

Hansen et. al. [21] reported the amount of a full monolayer of oxygen on each of the surfaces (111), (110) and (100) to be 1.82 x 10^{15} atoms/cm^2, 2.22 x 10^{15} atoms/cm^2 and 1.57 x 10^{15} atoms/cm^2 respectively. Since CVD diamond is polycrystalline, that is it

contains randomly oriented facets, the average of the full monolayer of oxygen for the above surfaces was taken, which was calculated to be 1.87 x 10^{15} atoms/cm^2. Using this value, the oxygen coverage of CVDBD4 was thus calculated to be 1.26 monolayers. The results obtained therefore confirm the presence of oxygen functionalities on the surface. An alternative technique that may be used to calculate the oxygen monolayer coverage is by altering the take-off angles for the electrons thereby giving them a geometrically longer path length [22]. Since the IMFP of electrons is quite small at Al K-alpha wavelengths, this method may be used to calculate monolayer coverages.

4.6 Contact angle measurements

4.6.1 Theory

The contact angle is a measure of the surface state, that is the hydrophilicity or hydrophobicity, of a solid sample. A hydrogen terminated diamond surface may be expected to be more hydrophobic, and an oxygen terminated surface more hydrophilic. Contact angle measurements were therefore used as a quick feedback method to evaluate the hydrogenation and oxygenation techniques used later in this work to modify the diamond surface. The two most widely used techniques to measure contact angles are the tensiometric method [23] and the drop method [21].

In a tensiometric method, the sample is suspended from an electrobalance and is slowly immersed into a liquid, for example water. The advancing angle is measured when the

sample is immersed into the aqueous solution and the receding angle is measured when the sample is extracted out of solution.

The drop method involves generating a droplet of water on the tip of a syringe and then applying the water droplet to the surface of the sample. If the drop completely wets the sample surface, the sample is said to be hydrophilic. If the droplet does not wet the surface, the sample is hydrophobic. To determine the hydrophobicity or hydrophilicity of the boron-doped CVD samples, the drop method was employed. It should be noted that the drop method is not a very accurate method and will only give an indication of the surface state of a sample by means of the contact angle measurement.

Figure 4.17 shows a schematic diagram of a droplet of water on the surface of a substrate. A low contact angle (θ) value implies a hydrophilic surface, whereas a high contact angle value implies a hydrophobic surface.

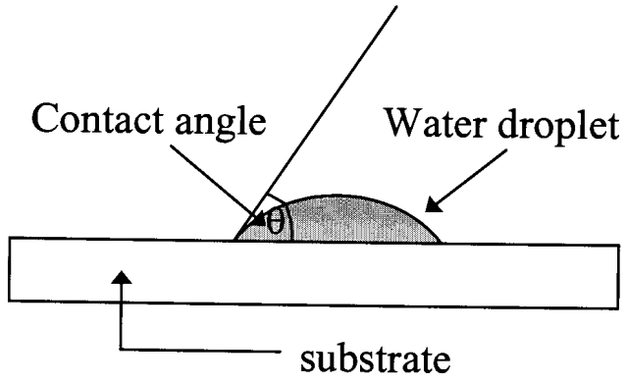

Figure 4.17 : Schematic diagram of a droplet of water on the surface of a substrate

4.6.2 Experimental and discussion

A Wild microscope (M420), prism and digital camera were used to measure the contact angles of the boron-doped CVD samples. A droplet of water was placed on the surface of the sample and, using a microscope, prism and a digital camera, an image representing the sideview of the sample was captured (**Figure 4.18**). Using a protractor, the contact angle for each sample was measured. A total of twenty measurements were taken for each sample and the average and standard deviation were calculated.

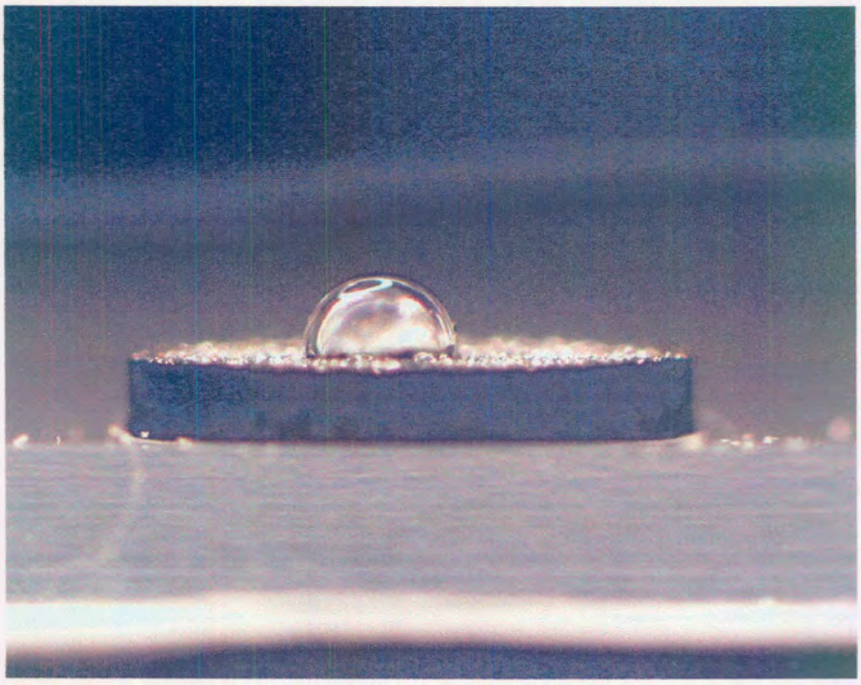

Figure 4.18 : Image of CVDBD2 containing a droplet of water

The results for the contact angle measurements are given in **Table 4.6**. The standard deviation for the respective measurements is quite high. Nevertheless, the differences

between the contact angles were sufficient to reveal a trend. It is evident from the contact angle measurements that CVDBD1 and CVDBD2 are hydrophobic, whilst CVDBD3 and CVDBD4 are partially hydrophobic. CVDBD5 and CVDBD6 tend to be more hydrophilic than the rest of the samples. It appears therefore that an increase in boron dopant level is accompanied by an increase in hydrophilicity, which indicates an increased presence of surface oxygen functionalities.

Table 4.6 : Contact angle measurements

CVD sample	Contact angle		
	Range / °	Average/ °	Std Deviation
CVDBD1 (undoped)	87 - 92	89.60	2.43
CVDBD2 (84 mg/L boron)	87 – 92	89.50	2.28
CVDBD3 (313 mg/L boron)	71 – 85	77.80	6.90
CVDBD4 (543 mg/L boron)	72 – 88	79.95	8.36
CVDBD5 (1032 mg/L boron)	54 – 67	60.50	6.15
CVDBD6 (1521 mg/L boron)	57 – 68	62.20	5.53

4.7 Resistance measurements

4.7.1 Experimental and discussion

In electrochemical applications, the electrode material should have a high conductivity (low resistance), in order to facilitate electron transport and to minimise the potential drop through the electrochemical cell. The total resistance (bulk and surface resistances) of the various boron-doped diamond samples was measured using a voltmeter and two copper electrodes. The copper electrodes were initially cleaned with hydrochloric acid to remove any passivating layer formed on the electrode surface. **Figure 4.19** illustrates the setup for the resistance measurements. The sample was placed between the two copper electrodes and a resistance measurement taken (**Figure 4.20**).

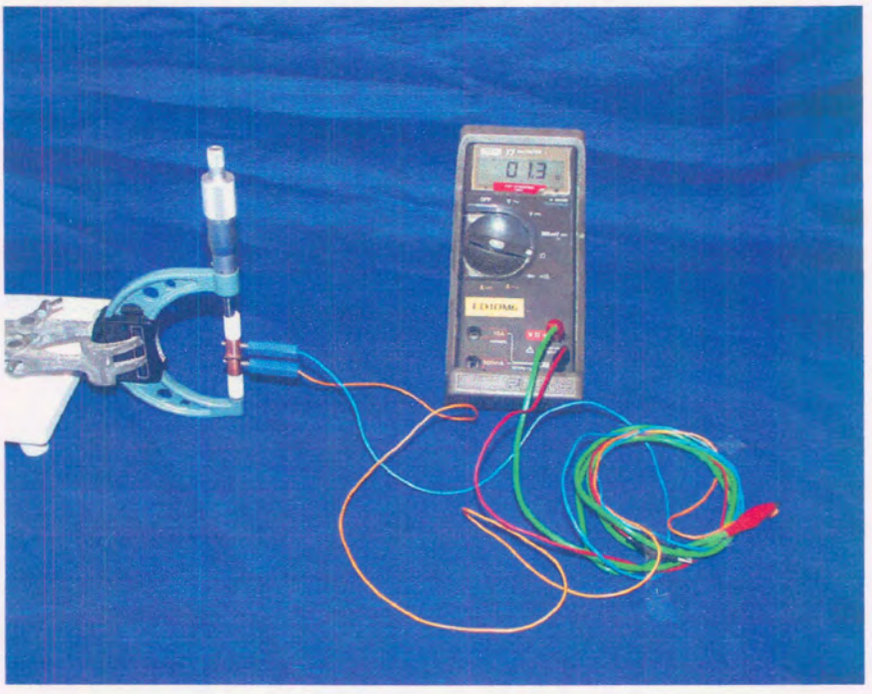

Figure 4.19 : Resistance measurement setup

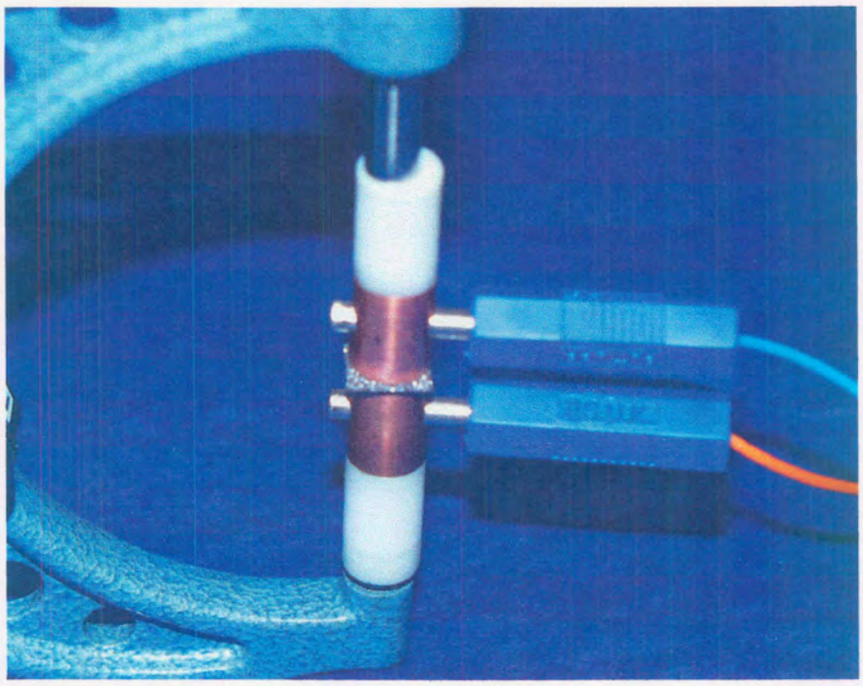

Figure 4.20 : Boron-doped CVD sample between two copper electrodes

Table 4.7 illustrates the resistance measurements of the various samples. CVDBD1 was found to have a resistance reading of mega Ω to overload. The conductivity of CVDBD2 and CVDBD3 seemed to be very low according to the resistance measurements, whilst the conductivity of CVDBD4 – CVDBD6 was found to be fairly high. From these measurements, it may be deduced that since CVDBD4 – CVDBD6 are fairly conductive, the minimum level of boron required to make diamond suitable as an electrode material is approximately 500 mg/L.

Table 4.7 : Resistance measurements of boron-doped CVD samples

CVD sample	Resistance / Ω
CVDBD1 (undoped)	-
CVDBD2 (84 mg/L boron)	1198 – 2183
CVDBD3 (313 mg/L boron)	74.20 – 214.18
CVDBD4 (543 mg/L boron)	1.02 – 1.43
CVDBD5 (1032 mg/L boron)	1.07 – 2.39
CVDBD6 (1521 mg/L boron)	2.29 – 3.77

As the boron concentration of the samples increases, the resistance of the samples should decrease. However, the resistance of CVDBD6 is higher than that of CVDBD4. According to the work carried out by Hansen et. al. [21], the resistance of diamond samples decreases as the hydrophobicity of the sample surfaces increase. Since CVDBD6 was found to be more hydrophilic than CVDBD4 (see **Section 4.6**), this could be a possible explanation of why CVDBD6 has a higher resistance than CVDBD4.

4.8 Conclusion

SEM analysis showed the surface of the boron-doped diamond samples to contain randomly oriented facets, whilst LA-ICP-MS measurements indicated that CVDBD2 contains the lowest boron concentration and CVDBD6 contains the highest boron concentration. According to the Raman spectroscopy analysis, the presence of boron in the sample appears to suppress the formation of sp^2 carbon. However, if the sample is doped with excessive amounts of boron, the amount of sp^2 carbon in the sample increases.

Using XPS, the oxygen content of CVDBD4 was found to be 2.37×10^{15} atoms/cm^2, with a surface oxygen coverage of 1.26 monolayers. The contact angle measurements revealed CVDBD1 and CVDBD2 to be hydrophobic, CVDBD3 and CVDBD4 to be partially hydrophobic and CVDBD5 and CVDBD6 to be more hydrophilic. And finally, the resistance measurements show CVDBD2 and CVDBD3 to have a low conductivity, whilst CVDBD4 – CVDBD6 were found to have a high conductivity. Thus, the minimum level of boron required to make diamond a suitable electrode material was found to be 500 mg/L.

4.9 References

[1] D Chescoe and P J Goodhew, **The Operation of Transmission and Scanning Electron Microscopes,** Oxford University Press (1990) 1.

[2] M C Granger, M Witek, J Xu, J Wang, M Hupert, A Hanks, M D Koppang, J E Butler, G Lucazeau, M Mermoux, J W Strojek and G M Swain, **Anal. Chem., 72** (2000) 3793.

[3] http://minerals.cr.usgs.gov/webdocs/icpms/laser.htm

[4] http://www.gfz-potsdam.de/pb4/pg3/equipment/laicpms.html

[5] H H Willard, L L Merritt, Jr., J A Dean, **Instrumental Methods of Analysis,** 5th Edition, D. Van Nostrand Company, New York, (1974) 189.

[6] S A Solin and A K Ramdas, **Phys. Rev. B 1** (1970) 1687.

[7] J Wagner, M Ramsteiner, C H Wild and P Koidl, **Phys. Rev., B 40** (1989) 1817.

[8] R J Nemanich, J T Glass, G Lucovsky and R E Shroder, **J. Vac. Sci. Technol., A 6** (1988) 1783.

[9] R E Schroder and R J Nemanich, **Phys. Rev., B 41** (1990) 3738.

[10] F Tuinstra and J L Koenig, **J. Chem. Phys., 53** (1970) 1126.

[11] M Yoshikawa, G Katagiri, H Ishida, A Ishitani and T Akamatsu, **Appl. Phys. Lett., 52** (1988) 1639.

[12] M Yoshikawa, N Nagai, M Matsuki, H Fukuda, G Katagiri, H Ishida and A Ishitani, **Phys. Rev., B 46** (1992) 7169.

[13] http://www-personal.umich.edu/~jshaver/virtual/explain.html

[14] P Bou and L Vandenbulcke, **J. Electrochem. Soc., 138** (1991) 2991.

[15] S R Sails, D J Gardiner, M Bowden, J Savage and D Rodway, **Diamond Relat. Mater., 5** (1996) 589.

[16] M C Polo, J Cifre and J Esteve, **Vacuum, 45** (1994) 1013.

[17] http://www.uksaf.org/tech/xps.html

[18] J M Walls, **Methods of surface analysis**, Cambridge University Press, Great Britian (1989).

[19] http://www.chem.qmw.ac.uk/surfaces/scc/scat5_3.htm

[20] http://www.chem.vt.edu/chem-ed/spec/material/xps.html

[21] J O Hansen, **Wetting of the Diamond Surface,** PhD Thesis, (1987).

[22] S Evans and C E Riley, **J. Chem. Soc., Faraday Trans. 2, 82** (1986) 541.

[23] J O Hansen, R G Copperthwaite, T E Derry and J M Pratt, **Journal of Colloid and Interface Science, 130** (1989) 347.

CHAPTER 5

Hydrogenation and oxygenation techniques

5.1 Introduction

The surface chemistry of boron-doped CVD diamond is deemed extremely important as far as the electrochemical behaviour of boron-doped diamond electrodes is concerned, i.e. the electrochemical response of the diamond electrode to several redox systems depends on the chemical surface state of the electrode. The chemical state of the boron-doped diamond electrode can be modified using hydrogenation and oxygenation techniques. Hydrogenation of the surface results in the surface becoming more hydrophobic due to the increased presence of hydrogen atoms (accompanied by an increase in the contact angle), whilst oxygenation of the surface results in the surface becoming more hydrophilic due to the increased presence of oxygen atoms (accompanied by a decrease in the contact angle).

5.1.1 Hydrogen treatment

According to the work carried out by Matsumoto et. al. [1], the most rapid thermal desorption of CO and CO_2 from diamond powders occurs at approximately 500°C. In addition, Hansen et. al. [2] suggests that the hydrogenation process, if carried out above

500°C, requires the desorption of a carbonyl group from the diamond surface, exposing a reactive surface carbon atom for hydrogenation, rather than the splitting of a C-O bond.

According to subsequent work carried out by Tapraeva et. al. [3], it was found that hydrogen treating a diamond sample at 20 – 300°C produced a layer of adsorbed hydrogen on the diamond surface. At 600 – 900°C, the hydrogen is chemically bound to the surface, and between 300 – 600°C, both forms of the hydrogen may be present. It is further stated that hydrogen can adsorb onto the diamond surface or chemically react with the oxygen-containing groups on the surface, leading to partial reduction (**Figure 5.1**) or replacement by hydrogen groups (**Figure 5.2**).

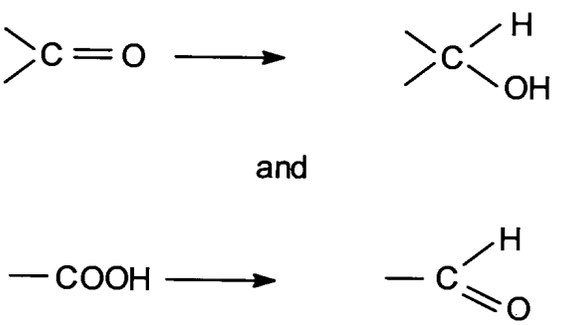

Figure 5.1 : Partial reduction of oxygen group

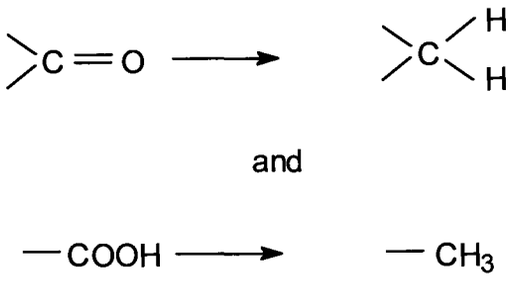

Figure 5.2 : Replacement by hydrogen groups

Examples of techniques for hydrogenation are :

(a) Heat treatment of the diamond samples in a tube furnace or a thermogravimetric analyser at 700°C under a flowing gas stream of either 10% hydrogen in argon or 99% hydrogen

(b) Hydrogen plasma treatment of the diamond sample

5.1.2 Oxygen treatment

Oxygen functional groups are always present on the surface of solids under normal conditions mostly due to exposure to air. These oxygen functional groups are chemisorbed on the carbon atoms, and are held very strongly by covalent bonds. As a result, a pure carbon surface can only be obtained and preserved for some time in an ultrahigh vacuum.

Various techniques exist for the attachment of oxygen functional groups onto a diamond surface. These are :

(a) Heat treatment of the diamond samples in a tube furnace or a thermogravimetric analyser between 260°C – 700°C in air or under a flowing gas stream of pure (99%) oxygen

(b) Heat treatment of the diamond samples in chromic acid, hydrogen peroxide or a mixture of sulphuric acid and potassium nitrate

(c) Anodisation of the diamond sample in a strong base, for example aqueous potassium hydroxide (KOH)

5.2 Hydrogenation techniques : experimental and discussion

5.2.1 Tube furnace treatment

A boron-doped CVD sample (CVDBD6(1)) was heat treated at 700°C in a tube furnace **(Figure 5.3)** under a flowing gas stream of 10% hydrogen in argon, for one hour. The contact angle of the sample was then measured **(Table 5.1)** and compared with the contact angle measured before furnace treatment. From a total of twenty contact angle measurements per sample, the average (Avg) and standard deviation (Std) were calculated. The decrease in the contact angle indicated that, in this experiment, the sample was in fact oxygenated instead of hydrogenated. This result may be ascribed to the presence of oxygen in the tube furnace during the reaction, either as an impurity in the feed gas, or due to insufficient sealing of the system. To prevent oxygen from the feed gas entering the system, an oxygen trap may be inserted in the gas line between the gas cylinder and the flow meter.

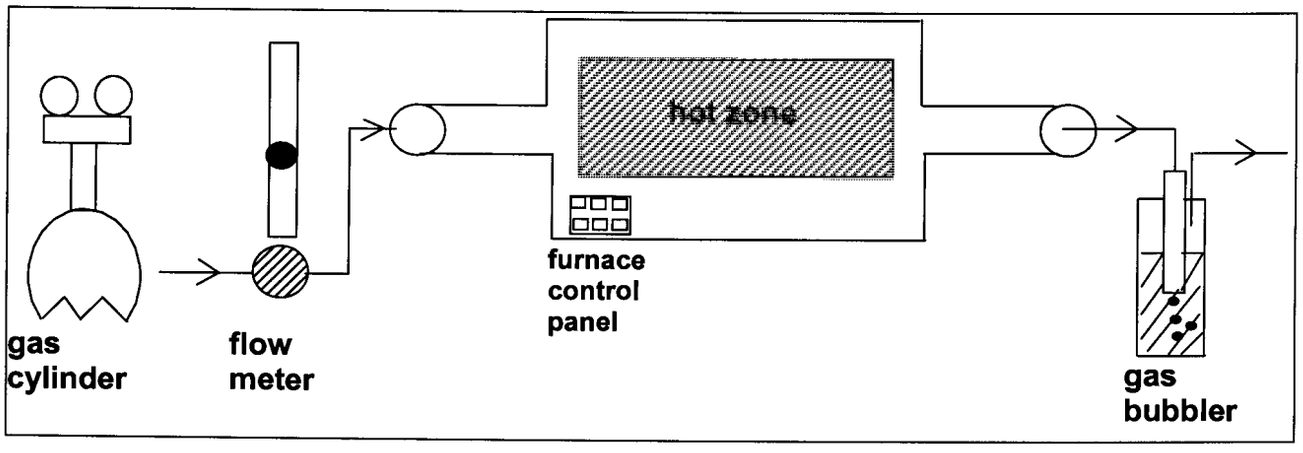

Figure 5.3 : Experimental tube furnace setup

To ensure that the surface of the sample is completely hydrogenated, 99% hydrogen can be used as the source gas. This system, however, becomes highly explosive if the system components and gas lines are not adequately sealed to prevent the escape of hydrogen into the atmosphere. To enable the safe running of the system, a hydrogen igniter may be installed at the end of the exhaust line.

Table 5.1 : Contact angle measurements : Hydrogenation

Diamond sample	Before hydrogenation	Hydrogenation technique		
		Tube furnace	TGA	Hydrogen plasma
CVDBD6(1)	Range : 57°-68° Avg : 62.2° Std : 5.53°	Range : 22°-35° Avg : 29.95° Std : 6.86°	-	-

CVDBD4(2)	Range : 66°-80° Avg : 73.1° Std : 6.96°	-	Range : 80°-91° Avg : 85.25° Std : 4.13°	-
CVDBD4	Range : 72°-88° Avg : 79.95° Std : 8.36°	-	-	Range : 88°-91° Avg : 89.78° Std : 1.22°

Avg : Average

Std : Standard deviation

5.2.2 Thermogravimetric analyser (TGA) treatment

The TGA apparatus is normally used to measure the mass change of a sample as a function of time. It consists of a six decimal place electronic balance with a weighing pan suspended in a small furnace. Some of the uses of a TGA include burn-off of organic matter, moisture determination and the oxidation and reduction temperature measurements of solid materials.

Since the furnace and sample chamber of the TGA are enclosed in a flowing gas stream, the problem of oxygen contamination from the surrounding atmosphere is eliminated. This makes the TGA more effective than the tube furnace for the hydrogenation of small samples.

A boron-doped CVD sample (CVDBD4(2)) was weighed into a platinum pan and the pan inserted into the TGA. The temperature was then ramped up to 700°C at 50°C/min and held there for two hours, under a flowing stream of 10% hydrogen in argon. The contact angle measurement of the sample after treatment is given in **Table 5.1**. This result confirmed that the TGA treatment is an effective method to obtain a hydrogenated surface.

5.2.3 Hydrogen plasma treatment

A standard microwave was converted into a hydrogen plasma treatment apparatus (**Figure 5.4**). A glass tube, which contained the sample, a thermocouple and a heating element was inserted into the centre of the microwave. Pure hydrogen (99%) was then introduced into the system. The microwaves that were generated by the microwave oven converted the hydrogen gas into hydrogen plasma. A mesh surrounding the tube helped prevent the escape of microwaves into the surrounding area and the cooling water helped absorb excess microwave radiation. For the microwave plasma treatment, the temperature was increased to 580°C at a pressure of 350 mTorr. The duration of the reaction was 30 minutes. The contact angle measurement after treatment **(Table 5.1)** suggests the hydrogen plasma treatment to be a very effective method for surface hydrogenation.

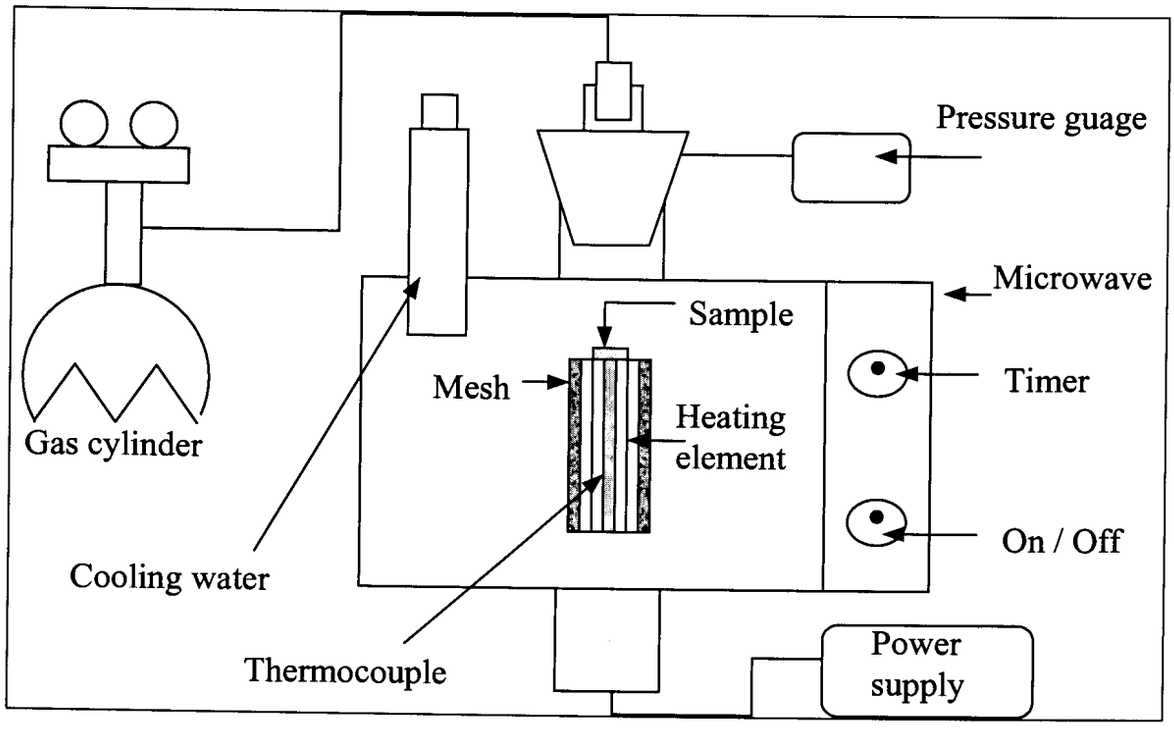

Figure 5.4 : Experimental setup of a microwave plasma apparatus

5.3 Oxygenation techniques : experimental and discussion

5.3.1 Chromic acid treatment

Chromic acid solution was prepared by the addition of 1 g of analytical grade potassium dichromate (obtained from Saarchem) to 20 ml of fuming sulphuric acid. CVDBD3 was then boiled in this solution for 30 minutes. Afterwards, contact angle measurements were taken **(Table 5.2)**, and the measurement showed that chromic acid treatment is very effective for obtaining hydrophilic diamond surfaces.

Table 5.2 : Contact angle measurements : Oxygenation

Diamond sample	Before oxygenation	After oxygenation	
		Chromic acid treatment	TGA
CVDBD3	Range : 71°-85° Avg : 77.80° Std : 6.90°	0°	-
CVDBD6(2)	Range : 57°-68° Avg : 62.20° Std : 5.53°	-	0°

However, it has one major drawback : during the acid treatment, chromium species are deposited onto the surface of the CVD sample, and this contamination subsequently occurs as a redox couple in the cyclic voltammogram of the CVD sample (see **Chapter 8**). The chromium species are removed on boiling the sample in hydrochloric acid for 10 minutes.

5.3.2 Anodisation treatment

The CVD sample (CVDBD4) which was obtained as a plate (length = 1 cm, width = 1 cm and thickness = 0.07 cm) from De Beers was laser cut (**Figure 5.5**) into smaller

circular discs to be used as working electrodes. The schematic construction of the diamond electrode is shown in **Figure 5.6**.

The electrode holder, which consisted of Teflon, was designed and manufactured for the easy insertion of a graphite insert. The laser cut diamond sample was subsequently glued onto the graphite insert using carbon paste. Electrical contact was made by the attachment of silver wire to the graphite insert via a screw thread. The assembled diamond electrode is shown in **Figure 5.7**.

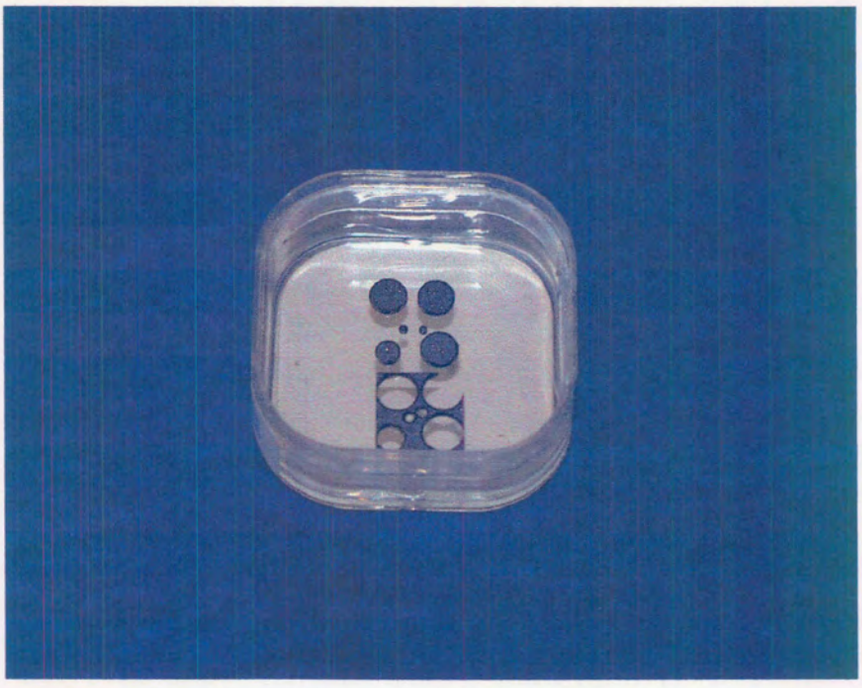

Figure 5.5 : Laser cut CVD sample

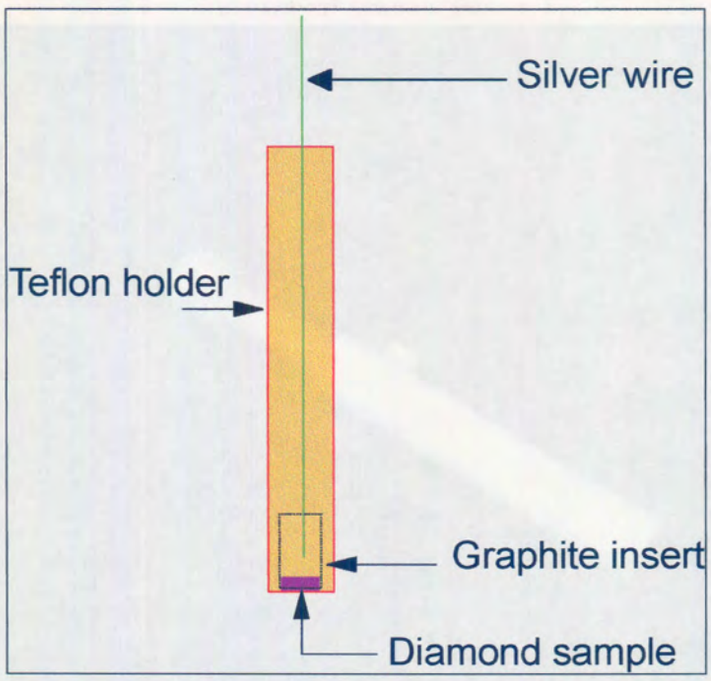

Figure 5.6 : Schematic construction of the diamond electrode

The diamond working electrode was then inserted into a three electrode electrochemical cell, containing 0.1 mol/L potassium hydroxide (KOH) (obtained from SMM Chemicals) solution. This cell was connected to an AutoLab PGStat 100 potentiostat. A constant potential of 2.7 V versus Ag/AgCl reference electrode was then applied to the boron-doped diamond electrode (BDD) for a period of 90 minutes. KOH was chosen for the anodisation reaction since it is a strong base.

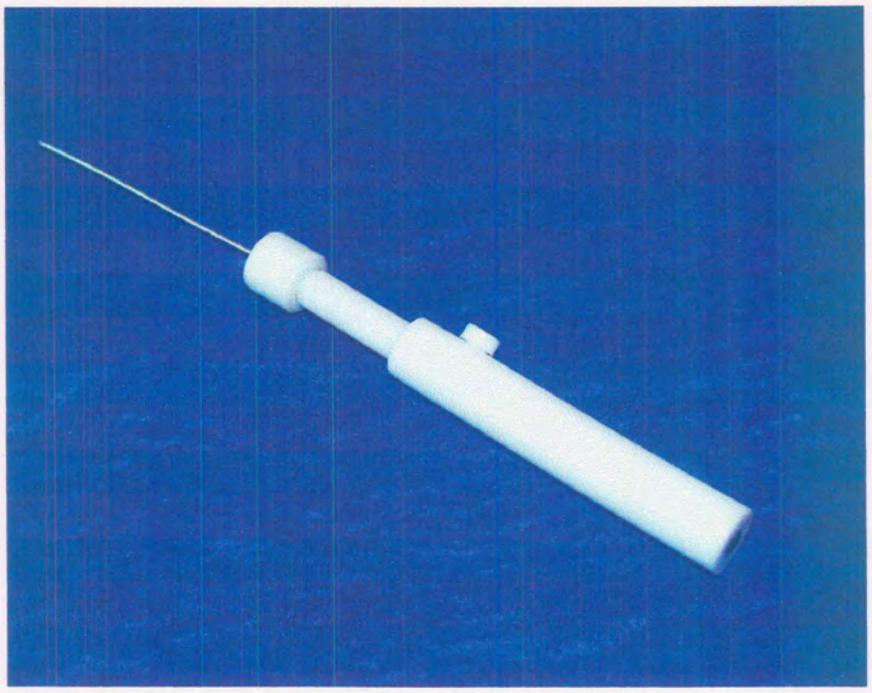

Figure 5.7 : Assembled diamond electrode

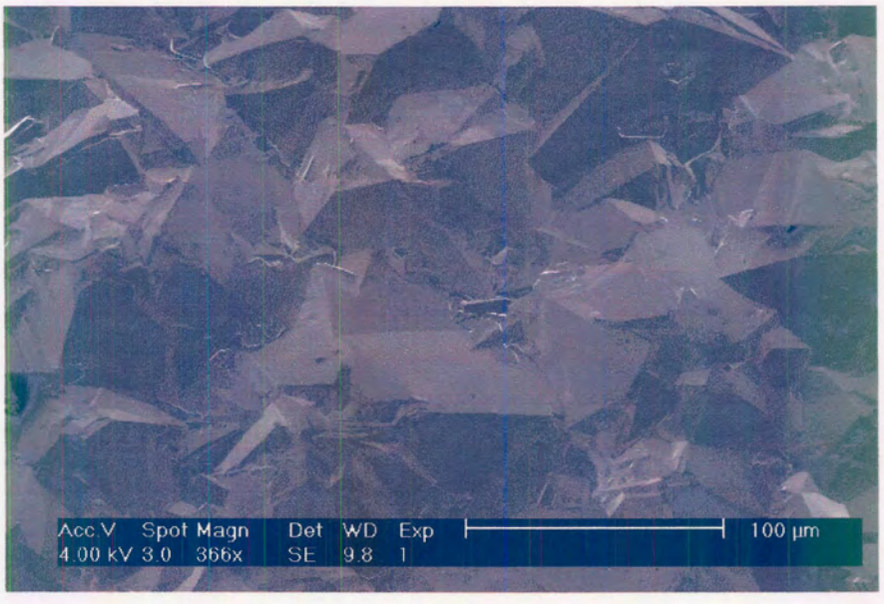

Figure 5.8 : SEM image of the as-received CVDBD4(2) sample

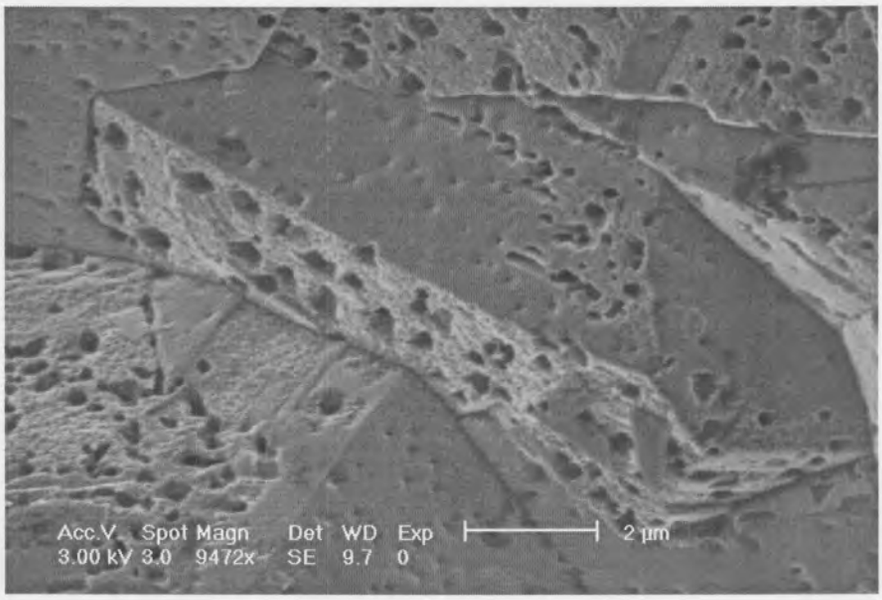

Figure 5.9 : SEM image of CVDBD4(2) after anodisation treatment

The SEM images of the CVD sample before and after treatment are shown in **Figure 5.8** and **Figure 5.9** respectively. Etch pits are apparent on the SEM image of the CVD sample after treatment. The oxygen content of the sample was subsequently analysed using XPS. **Figure 5.10** represents the XPS spectrum for the sample. A slight shift in the peak positions is observed in the treated sample as compared to the as-received sample (**Figure 4.16**). This could be attributed to the newly formed surface oxygen functionalities on the diamond surface.

The oxygen content as well as the oxygen coverage of the electrochemically treated sample and the as-received sample are shown in **Table 5.3**. It can be inferred from **Table 5.3** that a significant amount of oxygen atoms are either chemically or physically bound to the surface of the boron-doped CVD sample. The presence of these oxygen atoms renders the surface of the sample hydrophilic.

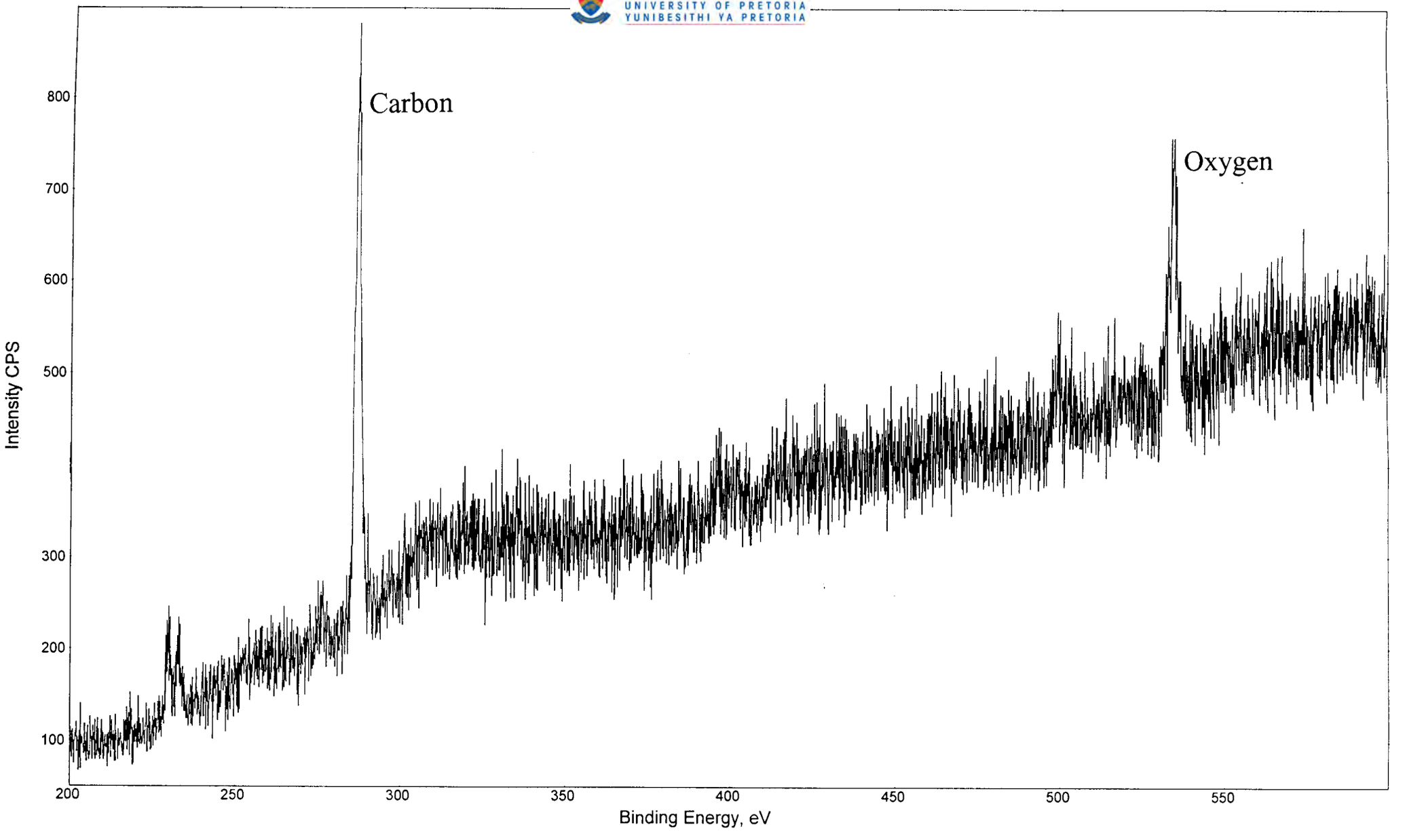

Figure 5.10 : XPS spectrum for CVDBD4(2) after anodisation

Table 5.3 : Oxygen content of boron-doped CVD samples

Diamond sample	Oxygen content / atoms.cm^{-2}	Surface oxygen coverage
CVDBD4(2) (as-received)	2.37 x 10^{15}	1.26 monolayers
CVDBD4(2) (anodised)	3.31 x 10^{15}	1.80 monolayers

5.3.3 Thermogravimetric analyser treatment

One of the undesirable characteristics of diamond is its susceptibilty to oxidation when heated. The onset of oxidation can occur at temperatures as low as 260°C [4]. Simons and Cannon [5] have reported that boron-doped diamond produced by the high pressure, high temperature (HPHT) process oxidised at 1/70 the rate of undoped HPHT diamond and at 1/100 the rate of a natural diamond. Further investigation of undoped CVD diamond [6-9] and boron-doped CVD diamond [10] confirmed that the boron-doping of CVD diamond decreases the oxidation rate of diamond.

In order to assess whether the boron-doping of De Beers CVD diamond decreases its oxidation rate, the work carried out by Farabaugh et. al. was repeated [10]. Two boron-doped CVD samples (CVDBD6 and CVDBD1, approximately 2 mg each) were weighed into a platinum pan and the pan inserted into the TGA. The temperature of the TGA was

programmed to increase from room temperature to 680°C at a rate of 50°C/min, and the temperature was then increased to 700°C at a rate of 20°C/min. The temperature was held at 700°C for five hours while high purity oxygen (99%) flowed through the sample chamber.

Figure 5.11 illustrates the TGA graph for the undoped (CVDBD1) and highest boron-doped (CVDBD6) samples. It is apparent from the two graphs that the total weight loss of the undoped sample is greater than that of the highest boron-doped sample. This observation confirms that boron-doping of CVD diamond decreases the oxidation rate of the diamond.

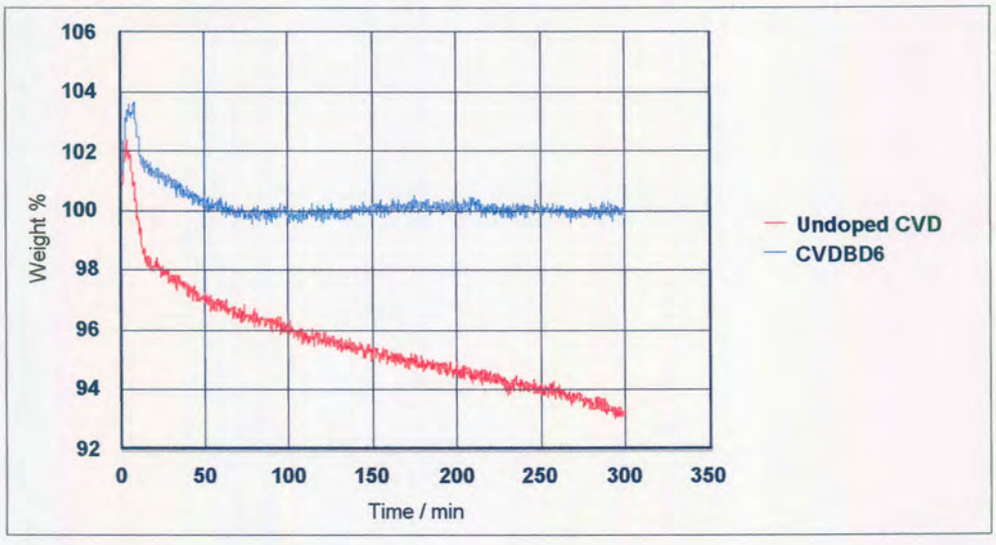

Figure 5.11 : TGA graph for the undoped and highest boron-doped sample (CVDBD6)

Farabaugh et. al. [10] further analysed the boron-doped CVD diamond residue from the TGA using Auger spectroscopy. They found an increase in the amount of oxygen and

boron on the CVD diamond surface. Furthermore, the boron peak shape very closely resembled the published boron peak shape in the Auger spectrum of boron oxide, indicating that during the oxidation of boron-doped CVD diamond, boron oxide is most likely formed on the diamond surface.

Assimilating the results as well as the suggestions reported in literature [1,3,6-9] and the results obtained in the current experiment, the following model for the oxidation of boron-doped CVD diamond may be proposed : when heating boron-doped CVD diamond in air, desorption of CO and CO_2 from the diamond surface begins at approximately 500°C. Oxygen atoms are initially chemisorbed onto the surface of the diamond, which contains tetrahedrally bonded carbon atoms and either a homogeneous or heterogeneous distribution of boron atoms. These oxygen atoms can then bind to the carbon atoms present to form oxygen functionalities on the surface of the diamond.

As the temperature increases to greater than 500°C, desorption of CO and CO_2 from the diamond surface occurs and an increase in the mass loss of the sample is observed **(Figure 5.11)**. As the carbon atoms together with the oxygen atoms begin to gasify and leave the surface, boron atoms become concentrated on the diamond surface. The boron atoms can then react with the incoming oxygen atoms to form boron oxide.

Literature suggests [10] that boron oxide forms a passivating layer on the diamond surface. This layer may inhibit the further reaction of oxygen atoms with carbon atoms to form CO and CO_2. The net result is a decrease in the mass loss of the sample as seen in

Figure 5.11. Further work needs to be done in order to verify the presence of boron oxide on the diamond surface after oxidation, using techniques such as Auger spectroscopy and X-ray diffraction. Whilst the presence of a passivating layer of boron oxide may be useful in reducing the rate of oxidation of the surface of boron-doped CVD diamond, this layer tends to decrease the conductivity of the sample. This may result in a poor electrochemical signal being observed.

5.4 Conclusion

The surface state of the CVD diamond electrode (i.e. whether it is hydrophilic or hydrophobic) affects the electrochemical behaviour of the electrode in various redox systems (see **Chapter 6** and **Chapter 7**). The most effective hydrogenation technique was found to be the hydrogen plasma treatment. The oxygenation of the diamond surface can easily be accomplished using the tube furnace, TGA, chromic acid and anodisation techniques.

Under a harsh oxygenation environment, for example temperatures greater than 700°C, etching, graphitisation as well as the formation of a boron oxide layer on the diamond surface may occur. This will drastically affect the observed electrochemical signal. The ideal oxygenation method for boron-doped CVD diamonds to be used as an electrode material would be one that yields oxygen functionalities on the surface of the electrode without the formation of a boron oxide passivating layer. A suitable oxygenation method could be to heat treat the CVD diamond in a tube furnace or TGA at temperatures below

250°C for a short period of time to minimise the formation of boron oxide. Alternatively, the CVD diamond can be mildly treated in hydrogen peroxide (H_2O_2).

5.5 References

[1] S Matsumoto, H Kanda, Y Sato and N Setako, **Carbon, 15** (1977) 299.

[2] J O Hansen, R G Copperthwaite, T E Derry and J M Pratt, **Journal of Colloid and Interface Science, 130** (1989) 347.

[3] F M Tapraeva, A N Pushkin, N I Epishina, I I Kulakova and A P Rudenko, **Russian Journal of Physical Chemistry, 60** (1986) 1092.

[4] H P Boehm, **Adv. Catalysis, 16** (1966) 219.

[5] E L Simons and P Cannon, **Nature (London), 210** (1996) 90.

[6] C E Johnson, M A S Hasting and W A Weimer, **J. Mater. Res., 5** (1990) 2320.

[7] M Alam and Q Sun, **J. Mater. Res., 8** (1993) 2870.

[8] A Joshi, R Nimmagadda and J Herrington, **J. Vac. Sci. Technol., A 8** (1990) 2137.

[9] K Tankala, T DebRoy and M Alam, **J. Mater. Res., 5** (1990) 2483.

[10] E N Farabaugh, L Robins and A Feldman, **J. Mater. Res., 10** (1995) 1448.